bioRxiv preprint doi: https://doi.org/10.1101/659805; this version posted June 4, 2019. The copyright holder for this preprint (which was not certified by peer review) is the author/funder. All rights reserved. No reuse allowed without permission.

IQSEC3 Mediates Npas4-dependent GABAergic Synaptic Transmission and Depressive-like Behavior

Seungjoon Kim[1,#], Dongseok Park[1,#], Dongsoo Lee[2,#], Sookyung Hong[3], Esther Yang[4], Jongcheol Jeon[3], Takuma Mori[5], Hyeonho Kim[1], Soo-Jeong Kim[1], Katsuhiko Tabuchi[5,6], Jaehoon Kim[3], Hyun Kim[4], Eunji Cheong[2,7], Ji Won Um[1,7,*] and Jaewon Ko[1,7,8,*]

[1]Department of Brain and Cognitive Sciences, Daegu Gyeongbuk Institute of Science and Technology (DGIST), 333 Techno Jungangdae-Ro, Hyeonpoong-myeon, Dalseong-gun, Daegu 42988, Korea

[2]Department of Biotechnology, College of Life Science and Biotechnology, Yonsei University, Seoul 03722, Korea

[3]Department of Biological Sciences, Korea Advanced Institute of Science and Technology (KAIST), Daejeon 34141, Korea

[4]Department of Anatomy, Korea University College of Medicine, Brain Korea 21 plus, Seoul 02841, Korea

[5]Department of Molecular and Cellular Physiology, Shinshu University School of Medicine, Matsumoto 390-8621, Japan

[6]Institute for Biomedical Sciences, Interdisciplinary Cluster for Cutting Edge Research, Shinshu University, Matsumoto 390-8621, Japan

[7]Co-Senior Authors

[8]Lead Contact

bioRxiv preprint doi: https://doi.org/10.1101/659805; this version posted June 4, 2019. The copyright holder for this preprint (which was not certified by peer review) is the author/funder. All rights reserved. No reuse allowed without permission.

[#]These authors contributed equally to this study

*Correspondence to Ji Won Um (jiwonum@dgist.ac.kr) or Jaewon Ko (jaewonko@dgist.ac.kr)

Keywords: Inhibitory synapse; Npas4; IQSEC3; Synaptic activity; GABA; ARF

bioRxiv preprint doi: https://doi.org/10.1101/659805; this version posted June 4, 2019. The copyright holder for this preprint (which was not certified by peer review) is the author/funder. All rights reserved. No reuse allowed without permission.

SUMMARY

Organization of mammalian inhibitory synapses is thought to be crucial for normal brain functions, but the underlying molecular mechanisms have remained largely undefined. IQSEC3, a guanine nucleotide exchange factor for ADP-ribosylation factor (ARF-GEF), is a component of γ-aminobutyric acid-producing (GABAergic) synapses that directly interacts with gephyrin. Here, we show that IQSEC3 (IQ motif and Sec7 domain 3) acts in a synaptic activity-dependent manner to regulate GABAergic synapse development *in vivo*. We found that Npas4 (neuronal PAS domain protein 4), a transcription factor that controls the number of GABAergic synapses formed on excitatory neurons, directly binds to the promoter of *Iqsec3* and regulates its transcription. Moreover, IQSEC3 functions downstream of Npas4 to orchestrate GABAergic synapse development. Strikingly, injection of mice with kainic acid (KA) induced Npas4 upregulation and concurrently increased IQSEC3 protein expression levels, especially in somatostatin (SST)-positive GABAergic interneurons in the hippocampal CA1 stratum oriens layer, which are blunted in Npas4 knockout (KO) mice. Furthermore, expression of wild-type (WT) IQSEC3, but not a dominant-negative (DN) ARF-GEF–inactive mutant, normalized the altered GABAergic synaptic transmission and formation on dendrites, but not the soma, of Npas4-deficient CA1 neurons. Lastly, expression of IQSEC3 WT, but not IQSEC3 DN, rescued the altered depressive behavior observed in mice in which Npas4 expression is disrupted in the

bioRxiv preprint doi: https://doi.org/10.1101/659805; this version posted June 4, 2019. The copyright holder for this preprint (which was not certified by peer review) is the author/funder. All rights reserved. No reuse allowed without permission.

CA1 region of the hippocampus. Collectively, our results suggest that IQSEC3 is a key GABAergic synapse component that is activated by Npas4 and ARF activity-dependent gene programs to orchestrate the functional excitation-to-inhibition balance.

Highlights:

- Npas4 binds the promoter of *IQSEC3* and regulates its expression.
- Npas4 upregulates IQSEC3 protein expression in somatostatin-positive interneurons.
- IQSEC3 is an Npas4 target that controls GABAergic synapse formation, transmission, and susceptibility to depression.
- The ARF-GEF activity of IQSEC3 is critical for its synaptic functions.

bioRxiv preprint doi: https://doi.org/10.1101/659805; this version posted June 4, 2019. The copyright holder for this preprint (which was not certified by peer review) is the author/funder. All rights reserved. No reuse allowed without permission.

INTRODUCTION

An essential function of the nervous system is to generate optimal behavioral responses to diverse environmental information; moreover, combinatorial interactions between genetic components and sensory cues are essential for driving discrete steps in brain development (Chen et al., 2017; Katz and Shatz, 1996; West and Greenberg, 2011; Wong and Ghosh, 2002). Neuronal activity and subsequent calcium influx activate specific signaling cascades that cause nuclear translocation of various transcription factors, resulting in the rapid induction of an early-response gene-expression program that, in turn, induces transcription of late-response genes that locally regulate synaptic development and plasticity. This paradigm has been well established at both glutamatergic-producing and γ-aminobutyric acid-producing (GABAergic) synapses (West and Greenberg, 2011; West et al., 2002). Transcription factors that are commonly induced by synaptic activity regulate distinct sets of target genes to control the strength, location, and number of both glutamatergic and GABAergic inputs (Mann and Paulsen, 2007). However, which specific transcription factors couple with key synapse-organizing proteins to orchestrate the regulation of synapse development at both transcriptional and post-transcriptional levels remains incompletely understood (West and Greenberg, 2011).

One prominent transcription factor that specifically controls GABAergic synapse development is Npas4 (neuronal PAS domain protein 4) (Bloodgood et al., 2013; Kim et al.,

bioRxiv preprint doi: https://doi.org/10.1101/659805; this version posted June 4, 2019. The copyright holder for this preprint (which was not certified by peer review) is the author/funder. All rights reserved. No reuse allowed without permission.

2018; Ko et al., 2015; Lin et al., 2008; Spiegel et al., 2014; Sun and Lin, 2016), which regulates neuronal excitability in the adult dentate gyrus (DG) and new and reactivated fear memories (Ploski et al., 2011; Sim et al., 2013). Npas4 recruits RNA polymerase II to promoters and enhancers of target genes that are regulated by neuronal activity in CA3 hippocampal subfields, thereby contributing to short- and long-term contextual memory (Ramamoorthi et al., 2011). Deletion of *Npas4* abolishes depolarization-induced mRNA expression of immediate-early genes, such as Arc/Arg3.1, c-Fos, Zif268/Egr1, and brain-derived neurotrophic factor (BDNF) (Ramamoorthi et al., 2011). Importantly, Npas4 expression levels dictate the degree of inhibition in specific neuronal compartments by organizing distinct neuron-type–specific genetic programs (Bloodgood et al., 2013; Spiegel et al., 2014). Notably, BDNF regulates somatic, but not dendritic, inhibition in neural circuits of CA1 pyramidal neurons, and is responsive only to increased inhibitory inputs in glutamatergic neurons (Bloodgood et al., 2013; Spiegel et al., 2014). In addition, Npas4 mediates experience-dependent spine development in olfactory bulb interneurons (INs) through control of Mdm2 expression, confers neuroprotection against kainic acid-induced excitotoxicity in hippocampal neurons through control of synaptotagmin-10 (Sy10) expression, and organizes the structure and strength of hippocampal mossy fiber-CA3 synapses during contextual memory formation through control of polo-like kinase 2 (Plk2) expression (Weng et al., 2018; Woitecki et al., 2016; Yoshihara et al., 2014).

bioRxiv preprint doi: https://doi.org/10.1101/659805; this version posted June 4, 2019. The copyright holder for this preprint (which was not certified by peer review) is the author/funder. All rights reserved. No reuse allowed without permission.

These prior studies suggest that synaptic roles of Npas4 vary in brain region- , synaptic- , and cellular context-dependent manner. Despite these insights, the sheer number of Npas4 target genes has hampered efforts to fully understand the mechanisms underlying Npas4-mediated GABAergic synapse development. IQSEC3 (IQ motif and Sec7 domain 3; also known as BRAG3 or SynArfGEF) was previously isolated as a putative Npas4 target (Bloodgood et al., 2013). However, direct functional coupling of Npas4 with IQSEC3 in the context of GABAergic synapse development *in vivo* has not been investigated.

Postsynaptic scaffolding proteins organize functional synapses, provide platforms for postsynaptic receptors, and regulate downstream signaling cascades (Arancibia-Carcamo and Moss, 2006; Fritschy et al., 2012). Arguably the most extensively studied scaffolding protein at GABAergic synapses is gephyrin (Choii and Ko, 2015; Papadopoulos and Soykan, 2011). We recently reported that gephyrin directly interacts with IQSEC3 to promote GABAergic synapse formation (Um, 2017; Um et al., 2016). IQSEC3, a member of the brefeldin A-resistant ADP ribosylation factor guanine exchange factor (ARF-GEF) family, is exclusively localized at GABAergic synapses (Fukaya et al., 2011; Sakagami et al., 2013; Um, 2017; Um et al., 2016). IQSEC3 overexpression increases the number of postsynaptic gephyrin and presynaptic GAD67 puncta, whereas IQSEC3 knockdown (KD) specifically decreases gephyrin cluster size in cultured hippocampal neurons, without altering gephyrin puncta density (Um et al., 2016).

bioRxiv preprint doi: https://doi.org/10.1101/659805; this version posted June 4, 2019. The copyright holder for this preprint (which was not certified by peer review) is the author/funder. All rights reserved. No reuse allowed without permission.

However, although the role of IQSEC3 *in vitro* has been investigated, the brain-region specific, neuronal activity-dependent role of IQSEC3 *in vivo* has yet to be identified.

Here, we provide the first evidence demonstrating that IQSEC3 is critical for GABAergic synapse development *in vivo*. Intriguingly, Npas4 binds to the promoter of *Iqsec3* to regulate *Iqsec3* expression levels in a manner that depends on various synaptic activity paradigms that concurrently increase Npas4 levels. Remarkably, KA-induced upregulation of IQSEC3 proteins is prominent in somatostatin (SST)-expressing interneurons in the hippocampal CA1 stratum oriens layer, suggesting a role for IQSEC3 in uniquely shaping hippocampal circuitries. Moreover, IQSEC3 regulates Npas4-dependent GABAergic synapse development. IQSEC3 further modulates the mode of Npas4-mediated GABAergic synaptic transmission in apical dendrites (but not soma) of CA1 pyramidal neurons, a function that also requires its ARF-GEF activity. Furthermore, CA1 expression of IQSEC3 WT, but not an ARF-GEF activity-deficient IQSEC3 mutant, restored the altered depressive behaviors observed in Npas4 knockout (KO) mice. However, apart from this Npas4-dependent IQSEC3 action in regulating the activity-dependent behavior of GABAergic neural circuits, IQSEC3 also acts as a universal GABAergic synapse organizer across other subcellular dendritic domains to exert Npas4-independent inhibition. On the basis of these results, we postulate that two mechanistic modes of IQSEC3 action underlie GABAergic synapse development: one links Npas4 activity to the IQSEC3-ARF

bioRxiv preprint doi: https://doi.org/10.1101/659805; this version posted June 4, 2019. The copyright holder for this preprint (which was not certified by peer review) is the author/funder. All rights reserved. No reuse allowed without permission.

complex, possibly in a specific type of GABAergic interneuron, and the other engages an Npas4-independent program in excitatory neurons, and possibly other types of GABAergic interneurons. We further suggest that IQSEC3 is a downstream factor for Npas4 in sculpting specific neuronal inhibition in distal dendritic domains by providing inhibitory inputs onto excitatory neurons, hinting at its crucial roles in shaping activity-dependent specific inhibitory neural circuits and controlling a selective set of mouse behaviors.

bioRxiv preprint doi: https://doi.org/10.1101/659805; this version posted June 4, 2019. The copyright holder for this preprint (which was not certified by peer review) is the author/funder. All rights reserved. No reuse allowed without permission.

RESULTS

IQSEC3 is Required for GABAergic Synapse Development *In Vivo.*

We previously reported that short hairpin RNA (shRNA)-mediated knockdown (KD) of IQSEC3 (IQSEC3 KD) had no impact on gephyrin-positive GABAergic synaptic puncta density, but reduced gephyrin puncta size in cultured hippocampal neurons (Um et al., 2016). To determine whether IQSEC3 is required for GABAergic synaptic transmission, we performed electrophysiology experiments in cultured hippocampal neurons using an IQSEC3 KD expression vector, established in our previous study (Um et al., 2016). IQSEC3 KD caused a significant decrease in the frequency, but not amplitude, of miniature inhibitory postsynaptic currents (mIPSCs) (**Figure S1A–S1C**). Re-expression of IQSEC3 in IQSEC3 KD neurons reversed the impaired GABAergic synaptic transmission (**Figure S1A–S1C**). In contrast, measurement of miniature excitatory postsynaptic currents (mEPSCs) showed that IQSEC3 KD did not alter excitatory synaptic transmission (**Figure S1D–S1F**). To extend these observations in neurons *in vivo*, we performed patch-clamp recordings in CA1 hippocampal pyramidal neurons from mice. *In utero* electroporation with short hairpin RNAs (shRNAs) targeting IQSEC3 (sh-IQSEC3) revealed that IQSEC3 KD specifically decreased the frequency, but not the amplitude, of mIPSCs without altering the frequency or amplitude of mEPSCs (**Figure 1A–**

bioRxiv preprint doi: https://doi.org/10.1101/659805; this version posted June 4, 2019. The copyright holder for this preprint (which was not certified by peer review) is the author/funder. All rights reserved. No reuse allowed without permission.

1G). Importantly, IQSEC3 KD did not alter the paired-pulse ratio of IPSCs (**Figure 1H, 1I**), suggesting that the IQSEC3 KD–induced reduction in GABAergic synaptic transmission reflects mainly postsynaptic effects. These results unambiguously demonstrate that the ARF-GEF activity of IQSEC3 is required for the selective regulation of GABAergic synaptic transmission by IQSEC3 *in vivo*.

IQSEC3 Orchestrates GABAergic Synapse Development in a Synaptic Activity- and ARF-GEF Activity-Dependent Manner.

Because GABAergic synapse development is known to be influenced by neural activity and experience (Hensch, 2005; Huang, 2009), we next asked whether promotion of GABAergic synapse development mediated by IQSEC3 also depends on GABA receptor-related signaling mechanisms. To this end, we transfected IQSEC3 WT or IQSEC3 KD expression vectors into cultured hippocampal neurons that were chronically treated (4–6 days) with 50 μM bicuculline, alone or together with 100 μM D-APV and 20 μM NBQX to block activity of $GABA_A$ and glutamate receptors, respectively. In control neurons, bicuculline treatment increased GABAergic synapse density, an effect that is likely induced by Npas4 upregulation (Lin et al., 2008); however, this effect was blunted in IQSEC3-overexpressing neurons (**Figure S3A**). Strikingly, IQSEC3 KD completely overrode the bicuculline effect on

bioRxiv preprint doi: https://doi.org/10.1101/659805; this version posted June 4, 2019. The copyright holder for this preprint (which was not certified by peer review) is the author/funder. All rights reserved. No reuse allowed without permission.

GABAergic synapse density; moreover, treatment with glutamate receptor antagonists also offset bicuculline and IQSEC3-overexpression effects on the puncta density of the GABAergic postsynaptic marker gephyrin (**Figure S3A, S3B**). Moreover, IQSEC3-overexpression effects on gephyrin or GAD67 puncta density were completely abrogated by treatment with either SecinH3 (an inhibitor of the cytohesin ARF-GEF family) or QS11 (an inhibitor of ARF-GAP [GTPase-activating protein]), both of which phenocopied ARF loss-of-function effects (Hafner et al., 2006; Kanamarlapudi et al., 2012) (**Figure S4**). These data support the idea that IQSEC3 organizes GABAergic synapse development in a synaptic activity-dependent manner, and further suggest that reciprocal cycling between GDP-bound inactive and GTP-bound active conformations of ARF is critical in this process.

Npas4 Binds to the *IQSEC3* Promoter.

Our observation that IQSEC3 is involved in activity-dependent GABAergic synapse development prompted us to investigate whether a GABAergic synapse-specific transcription factor controls this process by targeting IQSEC3. One prominent candidate factor with the potential to play this role is Npas4 (Lin et al., 2008; Shamloo et al., 2006). Npas4 orchestrates the expression of a wide variety of target genes, notably including that encoding BDNF, which regulates GABAergic synapse development to mediate domain-specific inhibition in particular

bioRxiv preprint doi: https://doi.org/10.1101/659805; this version posted June 4, 2019. The copyright holder for this preprint (which was not certified by peer review) is the author/funder. All rights reserved. No reuse allowed without permission.

cell-types (Bloodgood et al., 2013; Lin et al., 2008; Spiegel et al., 2014). Intriguingly, deep sequencing of Npas4-bound DNA revealed IQSEC3 as a putative Npas4 target (Bloodgood et al., 2013), and a recent genome-wide ChIP-seq analysis showed strong enrichment of Npas4 at the upstream region near the transcription start site of the *IQSEC3* gene (Kim et al., 2010) (**Figure 2A**). Intriguingly, we noted that this Npas4 peak contains a single Npas4 consensus CACG motif (**Figure 2A**). Thus, we tested whether IQSEC3, like BDNF, could also be an Npas4 target that acts to promote GABAergic synapse development. To this end, we cotransfected HEK293T cells with a *Iqsec3* promoter-luciferase reporter construct and a vector expressing Npas4. Ectopic expression of Npas4 increased luciferase expression ~3-fold; notably, this increase was abolished by mutation of the Npas4 consensus site in the *Iqsec3* promoter region (**Figure 2B**). Electrophoretic mobility shift assays (EMSAs) confirmed these results, showing that a radiolabeled *Iqsec3* WT oligoduplex probe containing purified Npas4 protein yielded a single bound complex; consistent with promoter-reporter assays, this DNA-protein interaction was abolished by mutation of the Npas4 consensus site (**Figure 2C**). Chromatin immunoprecipitation (ChIP) assays also demonstrated that Npas4 binds to the *Iqsec3* promoter in primary hippocampal cultured neurons treated with 55 mM KCl to trigger membrane depolarization (**Figure 2D**). No Npas4-binding was detected in untreated hippocampal cultured neurons (**Figure 2D**). These data suggest that Npas4 can function as a DNA-binding

bioRxiv preprint doi: https://doi.org/10.1101/659805; this version posted June 4, 2019. The copyright holder for this preprint (which was not certified by peer review) is the author/funder. All rights reserved. No reuse allowed without permission.

transcriptional activator of *IQSEC3*.

IQSEC3 Functions as an Npas4 Target to Promote GABAergic Synapse Development.

To further determine whether IQSEC3, analogous to BDNF (Lin et al., 2008), is involved in Npas4 actions on GABAergic synapse development, we infected cultured neurons with lentiviruses expressing shRNAs against *Iqsec3*, *Bdnf*, or control shRNA at 3 days *in vitro* (DIV3); transfected them at DIV10 with EGFP alone, or EGFP and myc-Npas4; and then immunostained them at DIV14 for gephyrin. Overexpression of Npas4 significantly increased gephyrin puncta density in both dendrites and soma, an effect that was completely abolished by IQSEC3 KD (**Figure 3A–3D**). These effects were distinct from the previously reported BDNF-KD effects on an Npas4 minigene, which led to altered GABAergic synaptic transmission specifically in the soma, but not in the dendritic compartment (Bloodgood et al., 2013) (**Figure 3A–3D**).

Next, to confirm that IQSEC3 functions downstream of Npas4, we tested whether IQSEC3 overexpression was capable of rescuing deficits in activity-induced GABAergic synapse development neurons lacking Npas4 (**Figure 3E, 3F)**. Cultured neurons transfected with Npas4 KD, IQSEC3 WT, or Npas4 KD plus IQSEC3 WT were treated with bicuculline to stimulate expression of endogenous Npas4 (**Figure 3E, 3F**). Npas4 KD significantly decreased

bioRxiv preprint doi: https://doi.org/10.1101/659805; this version posted June 4, 2019. The copyright holder for this preprint (which was not certified by peer review) is the author/funder. All rights reserved. No reuse allowed without permission.

the density of gephyrin puncta in Npas4 KD neurons, whereas IQSEC3 overexpression in these Npas4 KD neurons restored gephyrin puncta density to levels observed in control neurons (**Figure 3E, 3F**). These data reinforce the conclusion that IQSEC3 acts downstream of Npas4 to regulate activity-dependent GABAergic synapse development in cultured hippocampal neurons.

IQSEC3 Expression Level is Prominently Upregulated by Neuronal Activity *In Vivo* in SST-positive Interneurons of the Hippocampal CA1 Stratum Oriens.

To determine whether *Iqsec3* mRNA expression is changed in response to neuronal depolarization, similar to *Npas4* and *Bdnf* mRNAs, we depolarized cultured neurons infected with either control or Npas4 KD lentiviruses by incubation with 55 mM KCl for 2 hours, and then performed quantitative reverse transcription-polymerase chain reaction (qRT-PCR) (**Figure S5A**). Depolarization-induced *Npas4*, *Bdnf* and *Iqsec3* expression were consistently reduced in Npas4 KD neuron, compared with control neurons (**Figure S5A**). Blockade of synaptic activity using various receptor antagonists did not alter the mRNA levels of *Npas4, Bdnf, Iqsec3*, or *gephyrin* in cultured cortical neurons (**Figure S5B**). We next examined changes in IQSEC3 protein expression in adult mice in response to electroconvulsive seizure (ECS), which is known to promote neurogenesis and synaptogenesis, and has been used in the form of electroconvulsive therapy (ECT) to treat anti-depression through induction of a generalized

bioRxiv preprint doi: https://doi.org/10.1101/659805; this version posted June 4, 2019. The copyright holder for this preprint (which was not certified by peer review) is the author/funder. All rights reserved. No reuse allowed without permission.

seizure (Chen et al., 2009; Kaae et al., 2012; Kandratavicius et al., 2014). Protein levels of IQSEC3 and gephyrin (but not PSD-95) in both cortex and hippocampus, measured at 6 hours (but not at 3 hours) using semi-quantitative immunoblotting analyses, were significantly increased by ECS (**Figure S5C, S5D**). To further investigate the expression profile of IQSEC3 under network activity-altering conditions, we performed immunohistochemistry using ~11 week-old adult mice that were either injected with saline (SA) or 15 mg/kg of KA (**Figure 4A**). Consistent with a previous report (Bloodgood et al., 2013), KA injections significantly increased Npas4-positive cell numbers in both stratum pyramidale (SP) and stratum oriens (SO) layers of the hippocampal CA1 region, GCL and hilus of the DG (**Figure 4B**). Strikingly, KA injections resulted in an increase in the number of IQSEC3-positive cells, specifically in the SO layer, but not in the SP layer, molecular layer, or GCL of the DG (**Figure 4B, 4D**). Quantitative analyses using KA-injected floxed Npas4 mice ($Npas4^{f/f}$) expressing either active Cre-recombinase fused to EGFP (Cre) or inactive Cre-recombinase fused to EGFP (ΔCre, as a control) by AAV-mediated stereotactic injection showed that Npas4 deletions decreased the number of IQSEC3-positive cells to a level comparable to that observed in SA-injected WT mice (**Figure 4C, 4D**). Notably, the KA injection-dependent upregulation of IQSEC3 in the SO layer of the CA1 hippocampus was prominently observed in SST, but not parvalbumin (PV) or cholecystokinin (CCK), GABAergic interneurons (**Figure 4E, 4F**). We also addressed whether IQSEC3

bioRxiv preprint doi: https://doi.org/10.1101/659805; this version posted June 4, 2019. The copyright holder for this preprint (which was not certified by peer review) is the author/funder. All rights reserved. No reuse allowed without permission.

expression could be modulated by sensory input during postnatal development. To this end, we subjected mice to 5 days of dark rearing from P21 to P26, a period during which brain plasticity in visual cortical circuits is heightened (Hensch, 2004), and then re-exposed them to light for a brief period (2 hours) (**Figure S5E**). This dark rearing plus 2 hour-light (DR+2hL) paradigm induces rapid synaptic remodeling in the visual cortex and results in extensive molecular, functional, and structural synaptic changes (Lin et al., 2008; Peixoto et al., 2012). A 2 hour re-exposure to light after 5 days of dark rearing caused an enormous increase in *Npas4* mRNA level and a concomitant upregulation of *Iqsec3* and *gephyrin* mRNA expression (but not *Lrrtm3* mRNA expression) in the visual cortices of mice compared with the dark-reared group, as measured by qRT-PCR (**Figure S5E, S5F**) and RNAscope ISH (**data not shown**). In contrast, *Npas4*, *Iqsec3*, and *gephyrin* mRNA levels in hippocampus were unaltered in these mice (**Figure S5F**). Intriguingly, exposure of mice to an enriched environment induced *Iqsec3* and *gephyrin* mRNA expression, consistent with the observed increase in Npas4 expression level in response to an enriched environment (**data not shown**). Collectively, these data show that, although IQSEC3 mRNA expression increases in all layers of excitatory neurons examined using distinct experimental protocols, IQSEC3 protein levels are preferentially altered in specifically SST interneurons following KA-induced upregulation of network activity, following induction of neuronal activity *in vivo*.

bioRxiv preprint doi: https://doi.org/10.1101/659805; this version posted June 4, 2019. The copyright holder for this preprint (which was not certified by peer review) is the author/funder. All rights reserved. No reuse allowed without permission.

IQSEC3 is Required for Npas4-mediated GABAergic Synaptic Transmission in Dendrites of Hippocampal CA1 Pyramidal Neurons.

Because SST interneurons in the hippocampal CA1 oriens layer are known to regulate the activity of excitatory neurons through inhibition of the dendritic compartment of pyramidal neurons (Urban-Ciecko and Barth, 2016), and IQSEC3 is mainly postsynaptically expressed and promotes inhibitory synapse development (Um et al., 2016; this study), it is likely that IQSEC3 upregulation in SST interneurons would increase inhibitory inputs to SST interneurons. Thus, we next determined whether IQSEC3, as an Npas4 target, mediates inhibition of pyramidal neurons at specific subcellular compartments *in vivo*. To this end, we induced excision of Npas4 *in vivo* by injecting AAV-EGFP/Cre (Npas4 KO) into Npas4$^{f/f}$ mice; mice injected with AAV-EGFP/ΔCre served as controls. We then exposed these mice to an enriched environment for 4~5 days to induce Npas4 protein expression in pyramidal neurons and interneurons in the neuropil (**Figures 5A**), as previously described (Bloodgood et al., 2013; Hartzell et al., 2018), and recorded layer-specific, monosynaptically isolated, evoked inhibitory postsynaptic currents (eIPSCs) from AAV-infected CA1 pyramidal neurons (**Figure 5B–5I**). Consistent with a previous report (Bloodgood et al., 2013), stimulation of axons in the SP layer produced marginally, but significantly, smaller eIPSCs in Npas4 KO neurons than in neighboring Npas4

bioRxiv preprint doi: https://doi.org/10.1101/659805; this version posted June 4, 2019. The copyright holder for this preprint (which was not certified by peer review) is the author/funder. All rights reserved. No reuse allowed without permission.

WT neurons, whereas stimulation of axons in the stratum radiatum (SR) layer generated significantly larger eIPSCs in Npas4 KO neurons (**Figure 5B–5E**). Strikingly, expression of IQSEC3 WT in Npas4 KO neurons completely reversed the increase in eIPSC amplitude induced by stimulation of axons in the SR layer, but did not affect the decrease in eIPSC amplitude induced by stimulation of axons in the SP layer, compared with uninfected Npas4 KO neurons (**Figure 5F, 5G**). Expression of IQSEC3 E749A in Npas4 KO neurons did not affect the amplitudes of eIPSCs induced by stimulation of axons in the SR or SP layer (**Figure 5H, 5I**). Paired-pulsed ratios (PPRs) measured following stimulation of axons in SR and SP layers of Npas4 WT and Npas4 KO mice housed under enriched-environment conditions and infected with AAVs expressing IQSEC3 WT or IQSEC3 E749A were not different among groups (**Figure S6**), indicating that the Npas4-dependent changes in eIPSCs are not caused by altered presynaptic neurotransmitter release. These data indicate that Npas4 acts through IQSEC3 in a manner that depends on IQSEC3 ARF-GEF activity to mediate dendritic GABAergic synaptic inhibition *in vivo*.

To corroborate the electrophysiological data obtained from CA1 Npas4 KO neurons (**Figure 5B–5I**), we performed semi-quantitative analyses of endogenous $GABA_AR\gamma2$ puncta in the soma (SP layer), apical dendrites (SR layer), and basal dendrites (SO layer) of CA1 hippocampal neurons of $Npas4^{f/f}$ mice coinjected with AAVs encoding IQSEC3 WT and either

bioRxiv preprint doi: https://doi.org/10.1101/659805; this version posted June 4, 2019. The copyright holder for this preprint (which was not certified by peer review) is the author/funder. All rights reserved. No reuse allowed without permission.

EGFP-Cre (Npas4 KO) or EGFP-ΔCre (Control) (**Figure 5J**). Infected neurons were labeled by expressing AAV-EGFP-Cre or AAV-EGFP-ΔCre, whereas the differential effects of IQSEC3 expression in both somatic (SP layer) and dendritic (SR or SO layer) compartments on GABAergic synapse development were quantified by expressing AAV-IQSEC3 WT at moderate levels. The number of $GABA_AR\gamma2$ puncta in the SP layer of Npas4 KO neurons from mice exposed to enriched environment (EE) was significantly decreased compared with that in control neurons (**Figure 5K–5N**), with a concomitant increase in the number of apical dendritic $GABA_AR\gamma2$ puncta in the SR (but not SO) layer of Npas4 KO neurons, consistent with a previous report (Bloodgood et al., 2013). Remarkably, IQSEC3 WT expression in Npas4 KO neurons completely abrogated the increase in the density of $GABA_AR\gamma2$ puncta in the SR only in mice exposed to EE conditions, without altering SP $GABA_AR\gamma2$ puncta density (**Figure 5K–5N**), consistent with the electrophysiology data. However, IQSEC3 KD decreased the intensity of GAD67 puncta (but not VGLUT1 puncta) in all examined layers of hippocampal CA1 regions from mice under SE condition (**Figure S7**). These data suggest that IQSEC3 exerts differential Npas4 expression-independent inhibition *in vivo*.

IQSEC3 is Required for Hippocampal CA1- and Npas4-dependent Depressive Behavior.

Lastly, we investigated the behavioral effects of IQSEC3 expression in Npas4 KO mice.

bioRxiv preprint doi: https://doi.org/10.1101/659805; this version posted June 4, 2019. The copyright holder for this preprint (which was not certified by peer review) is the author/funder. All rights reserved. No reuse allowed without permission.

Npas4 KO mice have been reported to exhibit diverse cognitive, emotional, and social behavioral deficits (Heroux et al., 2018; Shepard et al., 2017; Sun and Lin, 2016; Weng et al., 2018). To link the hippocampal CA1 electrophysiological phenotypes in Npas4 KO mice with behavioral abnormalities, we performed a number of behavioral tasks, including elevated plus maze (EPM), Y-maze, open-field (OF), novel object-recognition (NOR), and forced swim (FS) tests using Npas4$^{f/f}$ mice injected with AAV-EGFP/ΔCre (Control), AAV-EGFP/Cre (Npas4 KO), or coinjected with AAV-EGFP/Cre and either IQSEC3 WT (+IQSEC3 WT), or IQSEC3 E749A (+IQSEC3 E749A), into the hippocampal CA1 region (**Figure 6A, 6B**). CA1 region-specific Npas4 KO mice exhibited decreased anxiety/exploration-related behavior (increased entries with similar time spent in open arms in the EPM test; **Figure S8**), enhanced locomotor activity (increased total distance traversed and velocity in the OF test; **Figure S9**), increased anti-depressive-like behavior (decreased immobility time in the FS test; **Figure 6C, 6D**), and moderately decreased working memory (decreased percentage of spontaneous alternation in the Y-maze test; **Figure 6E–6G**), but normal recognition memory (as assessed by the NOR test; **Figure S10**) phenotypes that are slightly different from those of constitutive Npas4 KO mice (Coutellier et al., 2012; Jaehne et al., 2015). Strikingly, expression of IQSEC3 WT was sufficient to rescue the increased anti-depressive-like behavior (FS test) and decreased working memory (Y-maze), but not the increased anxiety-related hyperactive behavior (EPM test), or

bioRxiv preprint doi: https://doi.org/10.1101/659805; this version posted June 4, 2019. The copyright holder for this preprint (which was not certified by peer review) is the author/funder. All rights reserved. No reuse allowed without permission.

locomotor-related hyperactive behavior (OF test) observed in CA1-specific Npas4 KO mice (**Figures 6C–6G** and **S8, S9**). Intriguingly, expression of IQSEC3 E749A produced a trend (albeit not significant) toward rescuing the decreased working memory (Y-maze test), but failed to normalize the increase in depressive-like behavior (FS test), suggesting that the ARF-GEF activity of IQSEC3 is selectively required for mediating the ability to form a subset of Npas4- and CA1-dependent mouse behaviors (**Figure 6C–6G**). Expression of BDNF in CA1-specific Npas4 KO mice induced enormous hyperactivity and anxiety, consistent with previous reports (Govindarajan et al., 2006; Kernie et al., 2000), thus, we were unable to perform Y-maze, EPM, or FS tests on BDNF-expressing CA1 Npas4 KO mice (**data not shown**; see **Figure S9**). Taken together, together with previous studies (Ramamoorthi et al., 2011; Weng et al., 2018), these data suggest that Npas4 employs distinct sets of downstream components in its roles in various types of cognitive tasks involving different brain regions.

bioRxiv preprint doi: https://doi.org/10.1101/659805; this version posted June 4, 2019. The copyright holder for this preprint (which was not certified by peer review) is the author/funder. All rights reserved. No reuse allowed without permission.

DISCUSSION

In this study, we provide evidence from various experimental approaches to support the conclusion that IQSEC3 organizes activity-dependent GABAergic synapse development and controls hippocampal CA1-dependent depressive-like behavior through intricate molecular mechanisms involving Npas4 and ARFs. The principal observations of the present study are as follows:

First, we provide the first *in vivo* demonstration that IQSEC3 is required for GABAergic synapse development in an ARF-GEF activity-dependent manner (**Figure 1**), consistent with the proposed mechanism identified in cultured hippocampal neurons (Um et al., 2016). IQSEC3 is indeed crucial for GABAergic synapse formation and transmission *in vivo* across diverse hippocampal subfields, as shown in extensive KD-based loss-of-function analyses in combination with rescue approaches. Notably, the ARF-GEF activity of IQSEC3 is required for most (if not all) functional assays employed in the current study, as shown by the inability of an IQSEC3 E749A missense mutant—an ARF-GEF activity-defective mutant of IQSEC3—to rescue various IQSEC3 KD phenotypes. In our previous study (Um et al., 2016), we proposed that the phenotype elicited by the IQSEC3 E749A mutant may be a gain-of-function phenotype because of differences in outcomes compared with IQSEC3 KD. However, how dysregulated ARF activity is directly involved in deficits in GABAergic synapse development remains

bioRxiv preprint doi: https://doi.org/10.1101/659805; this version posted June 4, 2019. The copyright holder for this preprint (which was not certified by peer review) is the author/funder. All rights reserved. No reuse allowed without permission.

unclear. Previous studies have focused on several ARF-GEFs as regulators of glutamatergic synaptic functions and dendrite developmental process. For example, ARNO (ARF nucleotide-binding site opener)/cytohesin-2, msec7-1/cytohesin-1, and EFA6A (exchange factor for ARF6), coupled with ARF6 functions, are involved in endosomal dynamics, dendritic outgrowth, branching, arborization, and spine development in neurons (Choi et al., 2006; Hernandez-Deviez et al., 2002; Huh et al., 2003). Moreover, GIT1 (G protein-coupled receptor kinase-interactor 1) regulates glutamate receptor trafficking, neurotransmitter release strength, and dendritic spine morphogenesis (Ko et al., 2003a; Montesinos et al., 2015; Segura et al., 2007; Zhang et al., 2005). These studies have consistently emphasized the roles of ARFs in various aspects of glutamatergic synapse development. BIG3 (brefeldin A-inhibited guanine nucleotide exchange protein 3) was reported to specifically regulate GABAergic synaptic transmission (Liu et al., 2016). More recently, overexpression of a dominant-negative, GTP binding-defective ARF6-T27N mutant was shown to recapitulate the phenotype of IQSEC3 E749A in cultured neurons, exhibiting mismatched apposition of pre- and postsynaptic structures (Fruh et al., 2018), consistent with our data (**Figure S4**). These observations suggest the intriguing possibility that ARF signaling pathways are involved in modulating activity-dependent GABAergic synapse development. Future studies should determine whether endogenous ARFs are located at both glutamatergic and GABAergic synaptic sites, and whether other ARFs

bioRxiv preprint doi: https://doi.org/10.1101/659805; this version posted June 4, 2019. The copyright holder for this preprint (which was not certified by peer review) is the author/funder. All rights reserved. No reuse allowed without permission.

besides ARF6 are similarly involved in GABAergic synapse development.

Second, IQSEC3 is linked to Npas4-mediated post-transcriptional programs that orchestrate activity-dependent GABAergic synapse development. The normal function of IQSEC3 in regulating GABAergic synapse development requires intact synaptic activity (**Figure S3**). The activity-dependent regulation of IQSEC3 function and expression level prompted us to dissect how IQSEC3 is related to the previously elucidated mechanisms underlying activity-dependent GABAergic synapse development. A prime candidate was Npas4, a well-known transcription factor and putative upstream regulator of IQSEC3 (Bloodgood et al., 2013; Sun and Lin, 2016). Npas4 binds to the promoter region of *Iqsec3*, which contains Npas4 consensus binding sites; IQSEC3 protein, in turn, functions downstream of Npas4 in regulating GABAergic inhibition in both somatic and dendritic compartments of cultured hippocampal neurons (**Figures 2** and **3**). In addition, we found that neuronal depolarization increased *Npas4* expression levels in cultured neurons and concomitantly upregulated IQSEC3 (**Figure S5**). Strikingly, manipulation of synaptic activity *in vivo* dynamically and distinctively affected the mRNA and protein levels of IQSEC3 (**Figures 4** and **S5**), consistent with the idea that IQSEC3, whose corresponding gene is an Npas4 target, promotes activity-dependent GABAergic synapse development. This interpretation is further supported by the observations that increased *Iqsec3* mRNA levels in depolarized neurons were significantly attenuated by Npas4 KD, and

bioRxiv preprint doi: https://doi.org/10.1101/659805; this version posted June 4, 2019. The copyright holder for this preprint (which was not certified by peer review) is the author/funder. All rights reserved. No reuse allowed without permission.

upregulated IQSEC3 protein levels in SST-positive interneurons of the hippocampal CA1 SO layer were completely compromised in Npas4 KO neurons (**Figure 4** and **S5**). Notably, a subset of different activity-induction protocols failed to induce changes in IQSEC3 expression levels, despite the fact that the same protocols markedly induced upregulation of Npas4 expression (**Figure S5**; **data not shown**). This suggests that context-dependent regulatory mechanisms may underlie Npas4-mediated transcriptional and post-transcriptional control of IQSEC3 levels *in vivo* (Tyssowski et al., 2018).

Third, IQSEC3 performs its inhibitory actions, distinct from other known Npas4 downstream components that are involved in regulating neural circuit-wide homeostasis (BDNF and Homer1a), neuroprotective signaling (Syt10), and synaptic plasticity during memory formation (Plk2) across various brain regions, neuron types and synapse types (Shan et al., 2018; Spiegel et al., 2014; Weng et al., 2018; Woitecki et al., 2016). Loss of Npas4 function results in reduced GABAergic synapse density in both perisomatic and dendritic regions of cultured hippocampal neurons (Lin et al., 2008), and blunts the inhibitory mode, concurrent with an abnormal distribution of GABAergic synapses at both soma and apical dendrites of CA1 pyramidal neurons (Bloodgood et al., 2013). BDNF is specifically expressed in excitatory 'cortical' neurons and serves to specifically promote perisomatic inhibition of them, whereas Plk2 is strongly expressed in excitatory 'hippocampal' CA3 pyramidal neurons that regulate

bioRxiv preprint doi: https://doi.org/10.1101/659805; this version posted June 4, 2019. The copyright holder for this preprint (which was not certified by peer review) is the author/funder. All rights reserved. No reuse allowed without permission.

thorny excrescence structures at mossy fiber-CA3 synapses (Spiegel et al., 2014; Weng et al., 2018). Anatomical analyses in the current study revealed that IQSEC3 KD abolished the Npas4-induced increase in inhibitory synaptic puncta density at both perisomatic and apical dendritic regions of hippocampal cultured neurons, whereas IQSEC3 overexpression in Npas4 KO neurons resulted in selective restoration of altered inhibitory synaptic transmission and structure in apical dendritic regions in CA1 hippocampal pyramidal neurons (**Figures 1, 3** and **5**). This mechanism of IQSEC3 action is in stark contrast to the specific mode of action of BDNF and neuroligin-2 at perisomatic regions of hippocampal neurons (Bloodgood et al., 2013; Gibson et al., 2009; Lin et al., 2008). In contrast, IQSEC3 KD decreased GAD67 puncta intensity in all examined layers of the hippocampal CA1 region (**Figure S7**). These observations might be integrated under a scenario in which altered inhibitory synapse development in both somatic and dendritic compartments of IQSEC3-deficient neurons involves at least two distinct pathways *in vivo*: an Npas4-dependent IQSEC3 pathway that mediates dendritic inhibition (**Figure 7B**), and an Npas4-independent IQSEC3 pathway that mediates somatic inhibition (**Figure 7A**). Consistent with this speculation, activity-dependent upregulation of IQSEC3 was notable in SST interneurons (but not excitatory neurons) of the hippocampal CA1 region (**Figure 4**), suggesting that one plausible role of IQSEC3 in SST neurons is to increase inhibitory inputs onto them enabling Npas4 to manage optimal responses and enhance feedback inhibition of

bioRxiv preprint doi: https://doi.org/10.1101/659805; this version posted June 4, 2019. The copyright holder for this preprint (which was not certified by peer review) is the author/funder. All rights reserved. No reuse allowed without permission.

principal neurons within local neural circuits in a context-dependent fashion (**Figure 7**). Given that IQSEC3 is expressed in various types of interneurons (PV-positive, SST-positive, CCK-positive) in mouse hippocampal regions (**data not shown**), it is likely that IQSEC3 differentially shapes specific circuit features that modulate homeostatic plasticity at distinct principal neuron-interneuron synapses. Moreover, expression of IQSEC3 completely normalized the altered anti-depressive-like behavior of CA1-specific Npas4 KO mice (**Figure 6**), suggesting that a distinct set of factors downstream of Npas4 is required for the performance of a spectrum of hippocampus-dependent cognitive and behavioral tasks (e.g., IQSEC3 for CA1-dependent anti-depressive-like behavior, and BDNF and Plk2 for CA3-dependent contextual memory formation). Conditional transgenic mice in which IQSEC3 is selectively deleted in specific interneurons should be further analyzed to address how various neural circuits involving different cell types are altered in the context of the GABAergic synaptic functions of IQSEC3 proposed in the current study. This further study is especially meaningful given the implications of SST-positive GABAergic neurons in modulating anxiolytic brain states and major depressive disorders through the control of inhibition at specific synapse types formed in discrete neural circuits (Fee et al., 2017; Fuchs et al., 2017; Klausberger et al., 2003; Lin and Sibille, 2015).

In conclusion, our observations underscore the significance of biochemical complexes

bioRxiv preprint doi: https://doi.org/10.1101/659805; this version posted June 4, 2019. The copyright holder for this preprint (which was not certified by peer review) is the author/funder. All rights reserved. No reuse allowed without permission.

involving IQSEC3, Npas4, ARFs, and other components in organizing activity-dependent GABAergic synapse development.

bioRxiv preprint doi: https://doi.org/10.1101/659805; this version posted June 4, 2019. The copyright holder for this preprint (which was not certified by peer review) is the author/funder. All rights reserved. No reuse allowed without permission.

STAR★METHODS

Detailed methods are provided in the online version of this paper and include the following:

- **KEY RESOURCES TABLE**
- **CONTACT FOR REAGENT AND RESOURCE SHARING**
- **EXPERIMENTAL MODEL AND SUBJECT DETAILS**
  - Cell culture
  - Animals
- **METHOD DETAILS**
  - Construction of Expression Vectors
  - Antibodies
  - Luciferase-promoter Analysis
  - Electrophoretic Mobility Shift Assay
  - Chromatin Immunoprecipitation Assay
  - Chemicals
  - Neuron Culture, Transfections, Imaging, and Quantitation
  - AAV Production, Stereotactic Surgery, and Virus Injection

bioRxiv preprint doi: https://doi.org/10.1101/659805; this version posted June 4, 2019. The copyright holder for this preprint (which was not certified by peer review) is the author/funder. All rights reserved. No reuse allowed without permission.

SUPPLEMENTAL INFORMATION

Supplemental Information includes 10 figures and 2 tables and can be found with this article online.

ACKNOWLEDGMENTS

We are grateful to Drs. Michael Greenberg (Harvard Medical School, USA), Yingxi Lin (MIT, USA) and Hiroyuki Sakagami (Kitasato University, Japan) for kind gifts of Npas4, BDNF, and

bioRxiv preprint doi: https://doi.org/10.1101/659805; this version posted June 4, 2019. The copyright holder for this preprint (which was not certified by peer review) is the author/funder. All rights reserved. No reuse allowed without permission.

IQSEC3/SynArfGEF reagents. This study was supported by grants from the National Research Foundation of Korea (NRF) funded by the Ministry of Science and Future Planning (2016R1A2B2006821 to J.Ko; 2015R1C1A2A01052176 to J.W.U.; 2012M3A9C6049938 to J.Kim), the Brain Research Program through the NRF funded by the Ministry of Science, ICT & Future Planning (2017M3C7A1023470 to J.Ko and E.C.), the DGIST R&D Program of the Ministry of Science, ICT and Future Planning (2019010079 to J.W.U.) and the Korea Healthcare Technology R & D Project, funded by the Ministry for Health and Welfare Affairs, Republic of Korea (HI17C0080 to J.Ko; HI15C3026 to J.W.U.). The authors declare no competing financial interests.

AUTHOR CONTRIBUTIONS

J.W.U. and J.Ko conceived the project; S.K., D.P., D.L., S.H., E.Y., Hyeonho K., J.J., T.M. and J.W.U. performed the experiments; S.K., D.P., D.L., S.H., E.Y., J.J., T.M., K.T., J.Kim, Hyun K., E.C., J.W.U. and J.Ko analyzed the data; and J.Kim, E.C., J.W.U. and J.Ko wrote the manuscript. All authors read and commented on the manuscript.

DECLARATION OF INTERESTS

The authors declare no competing interests.

bioRxiv preprint doi: https://doi.org/10.1101/659805; this version posted June 4, 2019. The copyright holder for this preprint (which was not certified by peer review) is the author/funder. All rights reserved. No reuse allowed without permission.

REFERENCES

Arancibia-Carcamo, I.L., and Moss, S.J. (2006). Molecular organization and assembly of the central inhibitory postsynapse. Results Probl Cell Differ 43, 25-47.

Bloodgood, B.L., Sharma, N., Browne, H.A., Trepman, A.Z., and Greenberg, M.E. (2013). The activity-dependent transcription factor NPAS4 regulates domain-specific inhibition. Nature 503, 121-125.

Chen, F., Madsen, T.M., Wegener, G., and Nyengaard, J.R. (2009). Repeated electroconvulsive seizures increase the total number of synapses in adult male rat hippocampus. Eur Neuropsychopharmacol 19, 329-338.

Chen, L.F., Zhou, A.S., and West, A.E. (2017). Transcribing the connectome: roles for transcription factors and chromatin regulators in activity-dependent synapse development. J Neurophysiol 118, 755-770.

Choi, S., Ko, J., Lee, J.R., Lee, H.W., Kim, K., Chung, H.S., Kim, H., and Kim, E. (2006). ARF6 and EFA6A regulate the development and maintenance of dendritic spines. J Neurosci 26, 4811-4819.

Choii, G., and Ko, J. (2015). Gephyrin: a central GABAergic synapse organizer. Exp Mol Med 47, e158.

Coutellier, L., Beraki, S., Ardestani, P.M., Saw, N.L., and Shamloo, M. (2012). Npas4: a

bioRxiv preprint doi: https://doi.org/10.1101/659805; this version posted June 4, 2019. The copyright holder for this preprint (which was not certified by peer review) is the author/funder. All rights reserved. No reuse allowed without permission.

neuronal transcription factor with a key role in social and cognitive functions relevant to developmental disorders. PLoS One 7, e46604.

Fee, C., Banasr, M., and Sibille, E. (2017). Somatostatin-Positive Gamma-Aminobutyric Acid Interneuron Deficits in Depression: Cortical Microcircuit and Therapeutic Perspectives. Biol Psychiatry 82, 549-559.

Fritschy, J.M., Panzanelli, P., and Tyagarajan, S.K. (2012). Molecular and functional heterogeneity of GABAergic synapses. Cell Mol Life Sci 69, 2485-2499.

Fruh, S., Tyagarajan, S.K., Campbell, B., Bosshard, G., and Fritschy, J.M. (2018). The catalytic function of the gephyrin-binding protein IQSEC3 regulates neurotransmitter-specific matching of pre- and postsynaptic structures in primary hippocampal cultures. J Neurochem.

Fuchs, T., Jefferson, S.J., Hooper, A., Yee, P.H., Maguire, J., and Luscher, B. (2017). Disinhibition of somatostatin-positive GABAergic interneurons results in an anxiolytic and antidepressant-like brain state. Mol Psychiatry 22, 920-930.

Fukaya, M., Kamata, A., Hara, Y., Tamaki, H., Katsumata, O., Ito, N., Takeda, S., Hata, Y., Suzuki, T., Watanabe, M., *et al.* (2011). SynArfGEF is a guanine nucleotide exchange factor for Arf6 and localizes preferentially at post-synaptic specializations of inhibitory synapses. J Neurochem 116, 1122-1137.

Gibson, J.R., Huber, K.M., and Südhof, T.C. (2009). Neuroligin-2 deletion selectively decreases

bioRxiv preprint doi: https://doi.org/10.1101/659805; this version posted June 4, 2019. The copyright holder for this preprint (which was not certified by peer review) is the author/funder. All rights reserved. No reuse allowed without permission.

inhibitory synaptic transmission originating from fast-spiking but not from somatostatin-positive interneurons. J Neurosci 29, 13883-13897.

Govindarajan, A., Rao, B.S., Nair, D., Trinh, M., Mawjee, N., Tonegawa, S., and Chattarji, S. (2006). Transgenic brain-derived neurotrophic factor expression causes both anxiogenic and antidepressant effects. Proc Natl Acad Sci U S A 103, 13208-13213.

Hafner, M., Schmitz, A., Grune, I., Srivatsan, S.G., Paul, B., Kolanus, W., Quast, T., Kremmer, E., Bauer, I., and Famulok, M. (2006). Inhibition of cytohesins by SecinH3 leads to hepatic insulin resistance. Nature 444, 941-944.

Hartzell, A.L., Martyniuk, K.M., Brigidi, G.S., Heinz, D., Djaja, N.A., Payne, A., and Bloodgood, B.L. (2018). Npas4 recruits CCK basket cell synapses and enhances cannabinoid-sensitive inhibition in the mouse hippocampus. Elife 7.

Hensch, T.K. (2004). Critical period regulation. Annu Rev Neurosci 27, 549-579.

Hensch, T.K. (2005). Critical period plasticity in local cortical circuits. Nat Rev Neurosci 6, 877-888.

Hernandez-Deviez, D.J., Casanova, J.E., and Wilson, J.M. (2002). Regulation of dendritic development by the ARF exchange factor ARNO. Nat Neurosci 5, 623-624.

Heroux, N.A., Osborne, B.F., Miller, L.A., Kawan, M., Buban, K.N., Rosen, J.B., and Stanton, M.E. (2018). Differential expression of the immediate early genes c-Fos, Arc, Egr-1, and Npas4

bioRxiv preprint doi: https://doi.org/10.1101/659805; this version posted June 4, 2019. The copyright holder for this preprint (which was not certified by peer review) is the author/funder. All rights reserved. No reuse allowed without permission.

during long-term memory formation in the context preexposure facilitation effect (CPFE). Neurobiol Learn Mem 147, 128-138.

Huang, Z.J. (2009). Activity-dependent development of inhibitory synapses and innervation pattern: role of GABA signalling and beyond. J Physiol 587, 1881-1888.

Huh, M., Han, J.H., Lim, C.S., Lee, S.H., Kim, S., Kim, E., and Kaang, B.K. (2003). Regulation of neuritogenesis and synaptic transmission by msec7-1, a guanine nucleotide exchange factor, in cultured Aplysia neurons. J Neurochem 85, 282-285.

Jaehne, E.J., Klaric, T.S., Koblar, S.A., Baune, B.T., and Lewis, M.D. (2015). Effects of Npas4 deficiency on anxiety, depression-like, cognition and sociability behaviour. Behav Brain Res 281, 276-282.

Kaae, S.S., Chen, F., Wegener, G., Madsen, T.M., and Nyengaard, J.R. (2012). Quantitative hippocampal structural changes following electroconvulsive seizure treatment in a rat model of depression. Synapse 66, 667-676.

Kanamarlapudi, V., Thompson, A., Kelly, E., and Lopez Bernal, A. (2012). ARF6 activated by the LHCG receptor through the cytohesin family of guanine nucleotide exchange factors mediates the receptor internalization and signaling. J Biol Chem 287, 20443-20455.

Kandratavicius, L., Balista, P.A., Lopes-Aguiar, C., Ruggiero, R.N., Umeoka, E.H., Garcia-Cairasco, N., Bueno-Junior, L.S., and Leite, J.P. (2014). Animal models of epilepsy: use and

bioRxiv preprint doi: https://doi.org/10.1101/659805; this version posted June 4, 2019. The copyright holder for this preprint (which was not certified by peer review) is the author/funder. All rights reserved. No reuse allowed without permission.

limitations. Neuropsychiatr Dis Treat 10, 1693-1705.

Katz, L.C., and Shatz, C.J. (1996). Synaptic activity and the construction of cortical circuits. Science 274, 1133-1138.

Kernie, S.G., Liebl, D.J., and Parada, L.F. (2000). BDNF regulates eating behavior and locomotor activity in mice. EMBO J 19, 1290-1300.

Kim, J., Guermah, M., McGinty, R.K., Lee, J.S., Tang, Z., Milne, T.A., Shilatifard, A., Muir, T.W., and Roeder, R.G. (2009). RAD6-Mediated transcription-coupled H2B ubiquitylation directly stimulates H3K4 methylation in human cells. Cell 137, 459-471.

Kim, S., Kim, H., and Um, J.W. (2018). Synapse development organized by neuronal activity-regulated immediate-early genes. Exp Mol Med 50, 11.

Kim, T.K., Hemberg, M., Gray, J.M., Costa, A.M., Bear, D.M., Wu, J., Harmin, D.A., Laptewicz, M., Barbara-Haley, K., Kuersten, S., *et al.* (2010). Widespread transcription at neuronal activity-regulated enhancers. Nature 465, 182-187.

Klausberger, T., Magill, P.J., Marton, L.F., Roberts, J.D., Cobden, P.M., Buzsaki, G., and Somogyi, P. (2003). Brain-state- and cell-type-specific firing of hippocampal interneurons in vivo. Nature 421, 844-848.

Ko, J., Choii, G., and Um, J.W. (2015). The balancing act of GABAergic synapse organizers. Trends Mol Med 21, 256-268.

bioRxiv preprint doi: https://doi.org/10.1101/659805; this version posted June 4, 2019. The copyright holder for this preprint (which was not certified by peer review) is the author/funder. All rights reserved. No reuse allowed without permission.

Ko, J., Kim, S., Valtschanoff, J.G., Shin, H., Lee, J.R., Sheng, M., Premont, R.T., Weinberg, R.J., and Kim, E. (2003a). Interaction between liprin-alpha and GIT1 is required for AMPA receptor targeting. J Neurosci 23, 1667-1677.

Ko, J., Na, M., Kim, S., Lee, J.R., and Kim, E. (2003b). Interaction of the ERC family of RIM-binding proteins with the liprin-alpha family of multidomain proteins. J Biol Chem 278, 42377-42385.

Ko, J., Soler-Llavina, G.J., Fuccillo, M.V., Malenka, R.C., and Sudhof, T.C. (2011). Neuroligins/LRRTMs prevent activity- and Ca2+/calmodulin-dependent synapse elimination in cultured neurons. J Cell Biol 194, 323-334.

Ko, J., Yoon, C., Piccoli, G., Chung, H.S., Kim, K., Lee, J.R., Lee, H.W., Kim, H., Sala, C., and Kim, E. (2006). Organization of the presynaptic active zone by ERC2/CAST1-dependent clustering of the tandem PDZ protein syntenin-1. J Neurosci 26, 963-970.

Li, K., Zhou, T., Liao, L., Yang, Z., Wong, C., Henn, F., Malinow, R., Yates, J.R., 3rd, and Hu, H. (2013). betaCaMKII in lateral habenula mediates core symptoms of depression. Science 341, 1016-1020.

Lin, L.C., and Sibille, E. (2015). Somatostatin, neuronal vulnerability and behavioral emotionality. Mol Psychiatry 20, 377-387.

Lin, Y., Bloodgood, B.L., Hauser, J.L., Lapan, A.D., Koon, A.C., Kim, T.K., Hu, L.S., Malik,

bioRxiv preprint doi: https://doi.org/10.1101/659805; this version posted June 4, 2019. The copyright holder for this preprint (which was not certified by peer review) is the author/funder. All rights reserved. No reuse allowed without permission.

A.N., and Greenberg, M.E. (2008). Activity-dependent regulation of inhibitory synapse development by Npas4. Nature 455, 1198-1204.

Liu, T., Li, H., Hong, W., and Han, W. (2016). Brefeldin A-inhibited guanine nucleotide exchange protein 3 is localized in lysosomes and regulates GABA signaling in hippocampal neurons. J Neurochem 139, 748-756.

Mann, E.O., and Paulsen, O. (2007). Role of GABAergic inhibition in hippocampal network oscillations. Trends Neurosci 30, 343-349.

Martinelli, D.C., Chew, K.S., Rohlmann, A., Lum, M.Y., Ressl, S., Hattar, S., Brunger, A.T., Missler, M., and Südhof, T.C. (2016). Expression of C1ql3 in Discrete Neuronal Populations Controls Efferent Synapse Numbers and Diverse Behaviors. Neuron 91, 1034-1051.

Montesinos, M.S., Dong, W., Goff, K., Das, B., Guerrero-Given, D., Schmalzigaug, R., Premont, R.T., Satterfield, R., Kamasawa, N., and Young, S.M., Jr. (2015). Presynaptic Deletion of GIT Proteins Results in Increased Synaptic Strength at a Mammalian Central Synapse. Neuron 88, 918-925.

Papadopoulos, T., and Soykan, T. (2011). The role of collybistin in gephyrin clustering at inhibitory synapses: facts and open questions. Front Cell Neurosci 5, 11.

Peixoto, R.T., Kunz, P.A., Kwon, H., Mabb, A.M., Sabatini, B.L., Philpot, B.D., and Ehlers, M.D. (2012). Transsynaptic signaling by activity-dependent cleavage of neuroligin-1. Neuron

bioRxiv preprint doi: https://doi.org/10.1101/659805; this version posted June 4, 2019. The copyright holder for this preprint (which was not certified by peer review) is the author/funder. All rights reserved. No reuse allowed without permission.

76, 396-409.

Ploski, J.E., Monsey, M.S., Nguyen, T., DiLeone, R.J., and Schafe, G.E. (2011). The neuronal PAS domain protein 4 (Npas4) is required for new and reactivated fear memories. PLoS One 6, e23760.

Ramamoorthi, K., Fropf, R., Belfort, G.M., Fitzmaurice, H.L., McKinney, R.M., Neve, R.L., Otto, T., and Lin, Y. (2011). Npas4 regulates a transcriptional program in CA3 required for contextual memory formation. Science 334, 1669-1675.

Sakagami, H., Katsumata, O., Hara, Y., Tamaki, H., Watanabe, M., Harvey, R.J., and Fukaya, M. (2013). Distinct synaptic localization patterns of brefeldin A-resistant guanine nucleotide exchange factors BRAG2 and BRAG3 in the mouse retina. J Comp Neurol 521, 860-876.

Segura, I., Essmann, C.L., Weinges, S., and Acker-Palmer, A. (2007). Grb4 and GIT1 transduce ephrinB reverse signals modulating spine morphogenesis and synapse formation. Nat Neurosci 10, 301-310.

Shamloo, M., Soriano, L., von Schack, D., Rickhag, M., Chin, D.J., Gonzalez-Zulueta, M., Gido, G., Urfer, R., Wieloch, T., and Nikolich, K. (2006). Npas4, a novel helix-loop-helix PAS domain protein, is regulated in response to cerebral ischemia. Eur J Neurosci 24, 2705-2720.

Shan, W., Nagai, T., Tanaka, M., Itoh, N., Furukawa-Hibi, Y., Nabeshima, T., Sokabe, M., and Yamada, K. (2018). Neuronal PAS domain protein 4 (Npas4) controls neuronal homeostasis in

bioRxiv preprint doi: https://doi.org/10.1101/659805; this version posted June 4, 2019. The copyright holder for this preprint (which was not certified by peer review) is the author/funder. All rights reserved. No reuse allowed without permission.

pentylenetetrazole-induced epilepsy through the induction of Homer1a. J Neurochem 145, 19-33.

Shepard, R., Heslin, K., and Coutellier, L. (2017). The transcription factor Npas4 contributes to adolescent development of prefrontal inhibitory circuits, and to cognitive and emotional functions: Implications for neuropsychiatric disorders. Neurobiol Dis 99, 36-46.

Sim, S., Antolin, S., Lin, C.W., Lin, Y., and Lois, C. (2013). Increased cell-intrinsic excitability induces synaptic changes in new neurons in the adult dentate gyrus that require Npas4. J Neurosci 33, 7928-7940.

Spiegel, I., Mardinly, A.R., Gabel, H.W., Bazinet, J.E., Couch, C.H., Tzeng, C.P., Harmin, D.A., and Greenberg, M.E. (2014). Npas4 regulates excitatory-inhibitory balance within neural circuits through cell-type-specific gene programs. Cell 157, 1216-1229.

Sun, X., and Lin, Y. (2016). Npas4: Linking Neuronal Activity to Memory. Trends Neurosci 39, 264-275.

Sztainberg, Y., and Chen, A. (2010). An environmental enrichment model for mice. Nat Protoc 5, 1535-1539.

Tyssowski, K.M., DeStefino, N.R., Cho, J.H., Dunn, C.J., Poston, R.G., Carty, C.E., Jones, R.D., Chang, S.M., Romeo, P., Wurzelmann, M.K., *et al.* (2018). Different Neuronal Activity Patterns Induce Different Gene Expression Programs. Neuron 98, 530-546 e511.

bioRxiv preprint doi: https://doi.org/10.1101/659805; this version posted June 4, 2019. The copyright holder for this preprint (which was not certified by peer review) is the author/funder. All rights reserved. No reuse allowed without permission.

Um, J.W. (2017). Synaptic functions of the IQSEC family of ADP-ribosylation factor guanine nucleotide exchange factors. Neurosci Res 116, 54-59.

Um, J.W., Choii, G., Park, D., Kim, D., Jeon, S., Kang, H., Mori, T., Papadopoulos, T., Yoo, T., Lee, Y., *et al.* (2016). IQ Motif and SEC7 Domain-containing Protein 3 (IQSEC3) interacts with gephyrin to promote inhibitory synapse formation. J Biol Chem.

Urban-Ciecko, J., and Barth, A.L. (2016). Somatostatin-expressing neurons in cortical networks. Nat Rev Neurosci 17, 401-409.

Weng, F.J., Garcia, R.I., Lutzu, S., Alvina, K., Zhang, Y., Dushko, M., Ku, T., Zemoura, K., Rich, D., Garcia-Dominguez, D., *et al.* (2018). Npas4 Is a Critical Regulator of Learning-Induced Plasticity at Mossy Fiber-CA3 Synapses during Contextual Memory Formation. Neuron 97, 1137-1152 e1135.

West, A.E., and Greenberg, M.E. (2011). Neuronal activity-regulated gene transcription in synapse development and cognitive function. Cold Spring Harb Perspect Biol 3.

West, A.E., Griffith, E.C., and Greenberg, M.E. (2002). Regulation of transcription factors by neuronal activity. Nat Rev Neurosci 3, 921-931.

Woitecki, A.M., Muller, J.A., van Loo, K.M., Sowade, R.F., Becker, A.J., and Schoch, S. (2016). Identification of Synaptotagmin 10 as Effector of NPAS4-Mediated Protection from Excitotoxic Neurodegeneration. J Neurosci 36, 2561-2570.

bioRxiv preprint doi: https://doi.org/10.1101/659805; this version posted June 4, 2019. The copyright holder for this preprint (which was not certified by peer review) is the author/funder. All rights reserved. No reuse allowed without permission.

Wong, R.O., and Ghosh, A. (2002). Activity-dependent regulation of dendritic growth and patterning. Nat Rev Neurosci 3, 803-812.

Xu, W., and Südhof, T.C. (2013). A neural circuit for memory specificity and generalization. Science 339, 1290-1295.

Yoshihara, S., Takahashi, H., Nishimura, N., Kinoshita, M., Asahina, R., Kitsuki, M., Tatsumi, K., Furukawa-Hibi, Y., Hirai, H., Nagai, T., *et al.* (2014). Npas4 regulates Mdm2 and thus Dcx in experience-dependent dendritic spine development of newborn olfactory bulb interneurons. Cell Rep 8, 843-857.

Zhang, H., Webb, D.J., Asmussen, H., Niu, S., and Horwitz, A.F. (2005). A GIT1/PIX/Rac/PAK signaling module regulates spine morphogenesis and synapse formation through MLC. J Neurosci 25, 3379-3388.

bioRxiv preprint doi: https://doi.org/10.1101/659805; this version posted June 4, 2019. The copyright holder for this preprint (which was not certified by peer review) is the author/funder. All rights reserved. No reuse allowed without permission.

FIGURE LEGENDS

Figure 1. IQSEC3 is Required for Inhibitory Synapse Development *In Vivo.*

(A) Neuronal precursors were transfected at E15 with IQSEC3 KD vectors by *in utero* electroporation. Coronal mouse brain sections were prepared at P14–P18. Numerous tdTomato-positive neurons were detected in the CA1 hippocampal region. Scale bar, 100 μm.

(B–D) Effect of IQSEC3 KD on inhibitory synaptic transmission in hippocampal CA1 pyramidal neurons. Representative traces **(B)** and summary graphs of the frequencies **(C)** and amplitudes **(D)** of mIPSCs in hippocampal CA1 pyramidal neurons transfected with Control or IQSEC3 KD are shown. Data represent means ± SEMs (*$p < 0.05$; Student's t-test); "n" denotes the total number of neurons recorded, as follows: Control, n = 9; and IQSEC3 KD, n = 9.

(E–G) Effect of IQSEC3 KD on excitatory synaptic transmission in hippocampal CA1 pyramidal neurons. Representative traces **(E)** and summary graphs of the frequencies **(F)** and amplitudes **(G)** of mEPSCs in hippocampal CA1 pyramidal neurons transfected with Control or IQSEC3 KD are shown. Data represent means ± SEMs (*$p < 0.05$; Student's t-test); "n" denotes the total number of neurons recorded, as follows: Control, n = 9; and IQSEC3 KD, n = 9.

(H and **I)** Effect of IQSEC3 KD on PPR (amplitude of the second IPSC divided by that of the first). Representative traces (**H**) and a summary graph (**I**) of PPR measured at 50-ms

bioRxiv preprint doi: https://doi.org/10.1101/659805; this version posted June 4, 2019. The copyright holder for this preprint (which was not certified by peer review) is the author/funder. All rights reserved. No reuse allowed without permission.

interstimulus intervals are shown. The data shown in the panels represent means ± SEMs; 'n' denotes the number of neurons recorded, as follows: Control, n = 8; and IQSEC3 KD, n = 8.

Figure 2. Npas4 Binds to the IQSEC3 Promoter in an Activity-dependent Manner.

(A) Schematic representation of the Iqsec3 locus indicating the three amplicons used for RT-qPCR. An Npas4-binding site identified by ChIP-seq analysis (Kim et al., 2010) is indicated as an Npas4 responsive element (Npas4 RE).

(B) HEK293T cells were cotransfected with a luciferase reporter construct (100 ng) containing a *Iqsec3* proximal promoter region (–280 to +36) together with a vector expressing Npas4 (40 ng), as indicated. MT indicates a promoter-reporter construct harboring a mutation in the consensus Npas4-binding sequence. Luciferase activity in cell extracts was assayed and expressed as relative to luciferase activity in cells transfected with a luciferase-reporter construct containing the WT *Iqsec3* promoter region (defined as 1). Values are expressed as means ± SEM from three independent experiments (***$p < 0.001$ vs. Mock-transfected controls; Mann-Whitney U Test).

(C) EMSAs employing purified FLAG-tagged Npas4 protein (10–90 ng) and a probe corresponding to nucleotide -110 to -69 within the *Iqsec3* proximal promoter are shown. An inset shows an image of a coomassie Blue-stained SDS-PAGE gel of the purified FLAG-Npas4 protein used in experiments.

bioRxiv preprint doi: https://doi.org/10.1101/659805; this version posted June 4, 2019. The copyright holder for this preprint (which was not certified by peer review) is the author/funder. All rights reserved. No reuse allowed without permission.

(D) ChIP-seq binding profiles for Npas4 at the *Iqsec3* locus in KCl-treated mouse cortical neurons. Data were downloaded from the GEO website (http://www.ncbi.nlm.nih.gov/geo); GEO accession number, GSE21161 (Kim et al., 2010). The total number of tags was normalized to the corresponding input.

Figure 3. IQSEC3 Mediates GABAergic Synapse Development as an Npas4 Target.

(A and **C)** Representative images of cultured hippocampal neurons infected at DIV3 with lentiviruses expressing EGFP alone (Control), IQSEC3 KD or BDNF KD, and transfected at DIV10 with lentiviral constructs expressing EGFP alone (Control) or cotransfected with EGFP and Npas4 (Npas4). Dendrites (**A**) or cell bodies (**C**) of transfected neurons were analyzed by double-immunofluorescence labeling for gephyrin (red) and EGFP (blue) at DIV14. Scale bar, 10 μm (applies to all images).

(B and **D)** Summary graphs of the effects of IQSEC3 KD or BDNF KD in Npas4-expressing neurons on gephyrin puncta density (left), gephyrin puncta size (middle), and gephyrin puncta intensity (right). Dendrites (**B**) and cell bodies (**D**) were quantified separately. For dendritic analyses, two or three dendrites per transfected neuron were chosen and group-averaged; n = 24 neurons/3 independent experiments. Data are presented as means ± SEMs (*$p < 0.05$; **$p <$

bioRxiv preprint doi: https://doi.org/10.1101/659805; this version posted June 4, 2019. The copyright holder for this preprint (which was not certified by peer review) is the author/funder. All rights reserved. No reuse allowed without permission.

0.01; non-parametric ANOVA with Kruskal-Wallis test, followed by *post hoc* Dunn's multiple comparison test).

(E) Representative images of cultured hippocampal neurons transfected at DIV8 with expression plasmids encoding EGFP (Control), *Npas4* shRNA vector (Npas4 KD), IQSEC3 or IQSEC3 plus Npas4 KD (Npas4 KD+IQSEC3), and analyzed at DIV14 by double-immunofluorescence staining with antibodies against gephyrin (red) and EGFP (blue). Bicuculline (50 μM) was added to cultured neurons at the time of transfection. Scale bar, 10 μm (applies to all images).

(F) Summary graphs of the effects of IQSEC3 overexpression on gephyrin puncta density, area, and intensity in Npas4 KD neurons. Dotted lines represent control levels for comparisons with other experimental conditions. Data are presented as means ± SEMs (*$p < 0.05$ vs. DMSO-treated controls; non-parametric ANOVA with Kruskal-Wallis test, followed by *post hoc* Dunn's multiple comparison test; n = 24 neurons/3 independent experiments).

Figure 4. IQSEC3 Protein Level is Regulated by Neuronal Activity *In Vitro* and *In Vivo.*

(A) Strategy employed in immunohistochemistry experiments presented in panels (**B–F**).

(B) Representative immunofluorescence images of hippocampal CA1 (*left*) and DG (*right*) regions from 11-week-old adult WT mice intraperitoneally injected with either SA or KA,

bioRxiv preprint doi: https://doi.org/10.1101/659805; this version posted June 4, 2019. The copyright holder for this preprint (which was not certified by peer review) is the author/funder. All rights reserved. No reuse allowed without permission.

immunostained for IQSEC3 (red) and Npas4 (green), and counterstained with DAPI (blue). Yellow arrows denote neurons in which IQSEC3 was upregulated by injection of KA, but not SA. Scale bar, 100 μm (left; CA1 *SO/SP*) and 200 μm (right; *DG*).

(C) Representative immunofluorescence images of hippocampal CA1 from Npas4$^{f/f}$ mice injected with AAVs expressing mCherry fused to inactive (ΔCre) or active (Cre) Cre recombinase at ~9 weeks of age, intraperitoneally injected with KA when mice at ~11 week old, and stained for IQSEC3 (green), ΔCre or Cre (red), and counterstained with DAPI (blue). Scale bar, 100 μm (applies to all images).

(**D)** Bar graphs summarizing quantitative results presented in (**B** and **C**). Abbreviations: DG, dentate gyrus; GCL, granule cell layer; K, kainic acid; ML, molecular layer; S, saline; SP, stratum pyramidale; SO, stratum oriens. Data are presented as means ± SEMs (*$p < 0.05$ vs. individual saline controls; Mann-Whitney *U* test; n = 24 sections/4 mice for all conditions).

(E) Representative immunofluorescence images of the hippocampal CA1 SO layer from 11-week old adult WT mice intraperitoneally injected with either SA or KA, immunostained for IQSEC3 (green), DAPI (blue), and SST (left), PV (middle), or CCK (right). Note that yellow arrows indicate the SST-positive interneurons with upregulated IQSEC3 levels. Scale bar, 50 μm (applies to all images).

(F) Bar graphs summarizing quantitative results presented in (**E**). Data are presented as means ±

bioRxiv preprint doi: https://doi.org/10.1101/659805; this version posted June 4, 2019. The copyright holder for this preprint (which was not certified by peer review) is the author/funder. All rights reserved. No reuse allowed without permission.

SEMs (*p < 0.05 vs. individual saline controls; Mann-Whitney *U* test; n = 18−24 sections/3−4 mice). Abbreviations: K, kainic acid; S, saline; SO, stratum oriens.

Figure 5. IQSEC3 Regulates Behaviorally Induced, Npas4-mediated Dendritic, But Not Somatic, Inhibition.

(A) Experimental configuration for *ex vivo* electrophysiology experiments. SL, stratum lacunosum; SR, stratum radiatum; SP, stratum pyramidale; and SO, stratum oriens.

(**B–I**) eIPSC measurements in mice exposed to enriched environment (EE). Representative traces (**B, D, F, H**) of responses in neurons infected with the indicated AAVs (blue or red) to stimulation in the SR or SP layer, normalized pairwise to responses in uninfected neighboring neurons (black). Quantification results are presented in (**C, E, G, I**). Open circles represent Npas4 KO/Npas4 WT pairs; black circles indicate means ± SEM (SR [blue]: Control (ΔCre), n = 7 pairs; Npas4 KO (Cre), n = 7 pairs; WT rescue (Cre + IQSEC3 WT), n = 9 pairs; E749A rescue (Cre + IQSEC3 E749A), n = 10 pairs. SP [red]: Control (ΔCre), n = 7 pairs; Npas4 KO (Cre), n = 7 pairs; WT rescue (Cre + IQSEC3 WT), n = 8 pairs; and E749A rescue (Cre + IQSEC3 E749A), n = 7 pairs). Data shown are means ± SEMs (*p < 0.05; paired two-tailed t-test). See **Table S2** for intrinsic electrophysiological properties of Npas4 WT and Npas4 KO neurons.

bioRxiv preprint doi: https://doi.org/10.1101/659805; this version posted June 4, 2019. The copyright holder for this preprint (which was not certified by peer review) is the author/funder. All rights reserved. No reuse allowed without permission.

(J) Experimental configuration for *in vivo* imaging experiments. SL, stratum lacunosum; SR, stratum radiatum; SP, stratum pyramidale; and SO, stratum oriens.

(K–N) Representative images (**K**) and quantification of dendritic $GABA_AR\gamma2$ puncta in the SO (**L**) or SR (**M**), and somatic $GABA_AR\gamma2$ puncta in the SP (**N**) of neurons obtained from mice housed under EE conditions and infected with either AAV-ΔCre-EGFP (Control), AAV-Cre-EGFP (Npas4 KO), or AAV-Cre-EGFP plus AAV-IQSEC3 WT (IQSEC3 WT res.). Data are presented as means ± SEMs (*$p < 0.05$; non-parametric ANOVA with Kruskal-Wallis test, followed by *post hoc* Dunn's multiple comparison test. n = 18–24 sections/3 mice for all conditions). Scale bar, 10 μm (applies to all images).

Figure 6. Expression of IQSEC3 WT, but Not IQSEC3 E749A, in the Hippocampal CA1 Normalizes Altered the Anti-depressive-like Behavior Observed in Npas4 KO Mice.

(A) Schematic diagram of mouse behavioral analyses. The CA1 region of the hippocampus of ~6 week Npas4 KO mice was bilaterally injected with AAVs expressing EGFP fused to inactive (ΔCre) or active (Cre) Cre recombinase, in combination with either of two IQSEC3 rescue AAVs—AAV-IQSEC3 WT (IQSEC3 WT res.) or AAV-IQSEC3 E749A (IQSEC3 E749A res.). Injected mice were subjected to five behavioral tasks 4 weeks after the injections in the

bioRxiv preprint doi: https://doi.org/10.1101/659805; this version posted June 4, 2019. The copyright holder for this preprint (which was not certified by peer review) is the author/funder. All rights reserved. No reuse allowed without permission.

indicated order. Abbreviations: EPM, elevated plus-maze test; FS, forced swim test; NOR, novel object-recognition test; and OF, open-field test.

(B) Representative brain section illustrating EGFP expression after AAV injection into the CA1. Scale bar, 100 μm.

(**C** and **D**) Analysis of the depressive-like behavior by FS test in Npas4$^{f/f}$ mice injected with the indicated AAVs. Immobility time (**C**) and latency to immobility (**D**) were measured. Data are presented as means ± SEMs (FS test: Control, n = 9; Npas4 KO, n = 9; Rescue [Npas4 KO (+IQSEC3 WT)], n = 8; and Rescue [Npas4 KO (+IQSEC3 E749A)], n = 7; *****p < 0.05; ******p < 0.01, one-way ANOVA with Bonferroni's *post-hoc* test).

(**E–G**) Analysis of the spatial working memory by Y-maze test in Npas4$^{f/f}$ mice injected with the indicated AAVs. Representative heat map showing movements of the indicated mice during the Y-maze test (**E**). Red represents increased time spent, and blue represents minimal time spent during the test. Spontaneous alternation performance ratio (% of spontaneous alternations; **F**) and total number of arm entries (**G**) were measured. Data are presented as means ± SEMs (Control, n = 12; Npas4 KO, n = 13; Rescue [Npas4 KO (+IQSEC3 WT)], n = 15; and Rescue [Npas4 KO (+IQSEC3 E749A)], n = 14; *****p < 0.05, one-way ANOVA with Bonferroni's *post-hoc* test).

bioRxiv preprint doi: https://doi.org/10.1101/659805; this version posted June 4, 2019. The copyright holder for this preprint (which was not certified by peer review) is the author/funder. All rights reserved. No reuse allowed without permission.

Figure 7. Molecular Model of IQSEC3 Action in Regulating Npas4 Activity-dependent Neural Circuit-wide Homeostasis.

(A) Npas4-independent IQSEC3 action in controlling activity-dependent GABAergic synapse development across universal synapse types. **(B)** Npas4-dependent IQSEC3 action in controlling activity-dependent GABAergic synapse development in specific synapse types. Neuronal activity-induced transcriptional programs are orchestrated by coordinated actions of various Npas4 downstream genes in distinct neuron types to maintain proper network activity. In WT mice (**B1**), a specific pattern of neuronal activity (①) specifically upregulates IQSEC3 expression in SST interneurons, possibly inducing increased inhibitory input onto SST interneurons (②), and act in conjunction with decreased inhibitory drive onto excitatory neurons to maintain circuit activity (③). This occurs despite widespread upregulation of Npas4 expression in both excitatory and inhibitory neurons, which may activate other Npas4 target genes in both excitatory and inhibitory neurons to maintain circuit activity. In contrast, neuronal activity fails to induce IQSEC3 upregulation in SST interneurons of Npas4 KO mice (**B2)** (④), possibly resulting in reduced recruitment of inhibitory inputs onto SST interneurons (⑤), and collectively contributing to increased inhibitory drive onto a specific dendritic domain in excitatory neurons (⑥), namely the dendritic domain in the SR layer, but not the SL or SO layer, of the hippocampal CA1 region).

bioRxiv preprint doi: https://doi.org/10.1101/659805; this version posted June 4, 2019. The copyright holder for this preprint (which was not certified by peer review) is the author/funder. All rights reserved. No reuse allowed without permission.

STAR★METHODS

KEY RESOURCES TABLE

REAGENT or RESOURCE	SOURCE	IDENTIFIER
Antibodies		
Rabbit polyclonal Anti-IQSEC3	Um et al., 2016	JK079; RRID: AB_2687864
Guinea pig Anti-IQSEC3/SynArfGEF	Fukaya et al., 2011	Clone #N6; RRID: AB_2314018
Rabbit polyclonal Anti-Npas4	Bloodgood et al., 2013	RRID: AB_2687869
Goat polyclonal Anti-Npas4	Abcam	Cat #ab109984; RRID: AB_10863874
Mouse monoclonal Anti-GAD67	Millipore	Cat #MAB5406; RRID: AB_2278725
Guinea pig polyclonal Anti-VGLUT1	Millipore	Cat #AB5905; RRID: AB_2301751
Mouse monoclonal Anti-Gephyrin	Synaptic Systems	Cat #147 011; RRID: AB_887717
Mouse monoclonal Anti-PSD-95	ThermoFisher Scientific	Cat #MA1-046; RRID: AB_2092361
Mouse monoclonal Anti-β-Actin	Santa Cruz Biotechnology	Cat #sc-47778; RRID: AB_626632
Mouse monoclonal Anti-PV	Swant	Cat #PV 235; RRID: AB_10000343
Mouse monoclonal Anti-SST	Millipore	Cat #MAB354; RRID: AB_2255365
Rabbit polyclonal Anti-CCK	Immunostar	Cat 20078; RRID: AB_572224
Goat polyclonal Anti-EGFP	Rockland	Cat #600-101-215; RRID: AB_218182
Cy3 conjugated Donkey Anti-Rabbit	Jackson ImmunoResearch Laboratories	Cat #711-165-152; RRID: AB_2307443
Cy3 conjugated Donkey Anti-Mouse	Jackson ImmunoResearch Laboratories	Cat #706-165-150; RRID: AB_2687868
Cy3 conjugated Donkey Anti-Guinea pig	Jackson ImmunoResearch Laboratories	Cat #706-165-148; RRID: AB_2340460

bioRxiv preprint doi: https://doi.org/10.1101/659805; this version posted June 4, 2019. The copyright holder for this preprint (which was not certified by peer review) is the author/funder. All rights reserved. No reuse allowed without permission.

FITC conjugated Donkey Anti-Mouse	Jackson ImmunoResearch Laboratories	Cat #715-035-150; RRID: AB_2340770
FITC conjugated Donkey Anti-Rabbit	Jackson ImmunoResearch Laboratories	Cat #711-095-152; RRID: AB_2315776
Chemicals, Peptides, and Recombinant Proteins		
Pentobarbital sodium	Sigma	Cat #P3761
Lipofectamine LTX Reagent with PLUS™ Reagent	ThermoFisher Scientific	Cat #15338100
Neurobasal medium	ThermoFisher Scientific	Cat #21103049
B-27 supplement (50X)	ThermoFisher Scientific	Cat #17504-044
Penicillin/Streptomycin	ThermoFisher Scientific	Cat #15140122
HBSS (Hanks' Balanced Salt Solution)	ThermoFisher	Cat #14065056
GlutaMax Supplement	ThermoFisher Scientific	Cat #35050061
Fetal Bovine Serum (FBS)	WELGENE	Cat #PK004-01
Sodium pyruvate	ThermoFisher Scientific	Cat #11360070
Poly-D-lysine hydrobromide	Sigma	Cat #P0899
SecinH3	Tocris	Cat #2849
QS11	Tocris	Cat #3324
Bicuculline	Tocris	Cat #0130
DL-2-amino-5-phosphonopentanoic acid (D-APV)	Tocris	Cat #0106
2,3-dihydroxy-6-nitro-7-sulfamoyl-benzo[f] quinoxaline-2,3-dione (NBQX)	Tocris	Cat #0373
6,7-Dinitroquinoxaline-2,3(1H,4H)-dione (DNQX)	Tocris	Cat #0189

bioRxiv preprint doi: https://doi.org/10.1101/659805; this version posted June 4, 2019. The copyright holder for this preprint (which was not certified by peer review) is the author/funder. All rights reserved. No reuse allowed without permission.

6-cyano-7-nitroquinoxaline-2,3-dione (CNQX)	Sigma	Cat #C239
QX-314	Tocris	Cat #1014
Tetrodoxin (TTX)	Tocris	Cat #1078
Potassium chloride (KCl)	ThermoFisher Scientific	Cat #7447-40-7
Picrotoxin	Sigma	Cat #P1675
Kainic acid	Sigma	Cat #K0250
Pilocarpine	Sigma	Cat #P6503
Methyl-scopolamine nitrate	Sigma	Cat #S2250
Poly(ethylene glycol; PEG)	Sigma	Cat #P5413
Ethanol	Millipore	Cat #1.00983.1011
Diazepam	Daewon Pharm	Cat #117
2,2,2-Tribromoethanol (Avertin)	Sigma	Cat #T48402
Tert-amylalcohol (Avertin)	Sigma	Cat #24048-6
Vectashield mounting medium	Vector Laboratories	Cat #H-1200
Critical Commercial Assays		
Sulfolink® Immobilization Kit for Proteins	ThermoFisher Scientific	Cat #44995
ReverTra Ace-α Kit	Toyobo	Cat #FSQ-301
CalPhos Transfection Kit	Takara	Cat #631312
Experimental Models: Cell Lines		
HEK 293T cells	ATCC	Cat # CRL-3216
Cultured neuronal cells (from rat embryos)	N/A	N/A
Experimental Models: Organisms/Strains		
Mouse: C57BL/6N	The Jackson Laboratory	Cat #005304
Mouse: *Npas4*$^{f/f}$	Bloodgood et al., 2013	RRID: MGI: 3828102
Recombinant DNA		
pAAV-U6-sh-IQSEC3-EGFP	This study	N/A
pAAV-U6-EGFP	Cell Biolabs	Cat #: VPK-413
L-315 sh-IQSEC3	Um et al., 2016	N/A
L-315 sh-Npas4	This study	N/A
L-315 sh-BDNF	This study	N/A

bioRxiv preprint doi: https://doi.org/10.1101/659805; this version posted June 4, 2019. The copyright holder for this preprint (which was not certified by peer review) is the author/funder. All rights reserved. No reuse allowed without permission.

pcDNA3 Myc-Npas4	Lin et al., 2008	N/A
pcDNA3.1 Myc-IQSEC3 WT	Um et al., 2016	N/A
pcDNA3.1 Myc-IQSEC3 E749A	Um et al., 2016	N/A
pAAV2/9-WGA-Cre-IRES-tdTomato	Martinelli et al., 2016	N/A
pAAV2/9-WGA-ΔCre-IRES-tdTomato	Martinelli et al., 2016	N/A
pAAV2/9-IQSEC3 WT	This study	N/A
pAAV2/9-IQSEC3 E749A	This study	N/A
pAAV2/9-BDNF	This study	N/A
pAAV2/9-Cre-IRES-EGFP	Xu et al., 2013	N/A
pAAV2/9-ΔCre-IRES-EGFP	Xu et al., 2013	N/A
Sequence-Based Reagents		
Iqsec3 rat probe (for qRT-PCR)	This study	N/A
Iqsec3 mouse probe (for qRT-PCR)	This study	N/A
Gephyrin rat probe (for qRT-PCR)	This study	N/A
Gephyrin mouse probe (for qRT-PCR)	This study	N/A
Npas4 rat probe (for qRT-PCR)	This study	N/A
Npas4 mouse probe (for qRT-PCR)	This study	N/A
Lrrtm3 rat probe (for qRT-PCR)	This study	N/A
Bdnf rat probe (for qRT-PCR)	This study	N/A
Software and Algorithms		
MetaMorph	Molecular Devices	https://www.moleculardevices.com/
ImageJ	NIH	https://imagej.nih.gov/ij/
GraphPad Prism 7.0	GraphPad	https://www.graphpad.com
Statistical Package for the Social Sciences 23 (SPSS 23)	IBM	https://www.ibm.com
Mini Analysis	Synaptosoft	https://www.synaptosoft.com/MiniAnalysis
EthoVision XT 10	Noldus	http://www.noldus.com/animal-behavior-research/products/ethovision-xt

bioRxiv preprint doi: https://doi.org/10.1101/659805; this version posted June 4, 2019. The copyright holder for this preprint (which was not certified by peer review) is the author/funder. All rights reserved. No reuse allowed without permission.

CONTACT FOR REAGENT AND RESOURCE SHARING

Further information and requests for resources and reagents should be directed to and will be fulfilled by the Lead Contact, Dr. Jaewon Ko (jaewonko@dgist.ac.kr).

EXPERIMENTAL MODEL AND SUBJECT DETAILS

Cell Culture

HEK293T cells were cultured in Dulbecco's Modified Eagle's Medium (DMEM; WELGENE) supplemented with 10% fetal bovine serum (FBS; Tissue Culture Biologicals) and 1% penicillin-streptomycin (Thermo Fisher) at 37°C in a humidified 5% CO_2 atmosphere. Cultured primary hippocampal neurons were prepared from embryonic day 18 (E18) Sprague-Dawley rat brains (KOATECK). Neurons were seeded on 25-mm poly-L-lysine (1 mg/ml)–coated coverslips and cultured in Neurobasal media (Gibco) containing penicillin-streptomycin and 0.5 mM GlutaMax (Thermo Fisher) supplemented with 2% B-27 (Thermo Fisher) and 0.5% FBS (Hyclone). All procedures were conducted according to the guidelines and protocols for rodent experimentation approved by the Institutional Animal Care and Use Committee of DGIST.

Animals

bioRxiv preprint doi: https://doi.org/10.1101/659805; this version posted June 4, 2019. The copyright holder for this preprint (which was not certified by peer review) is the author/funder. All rights reserved. No reuse allowed without permission.

All C57BL/6N mice were maintained and handled in accordance with protocols approved by the Institutional Animal Care and Use Committee of DGIST under standard, temperature-controlled laboratory conditions, or in an enriched environment with free access to colored tunnels, mazes, climbing materials, and running wheels. Mice were kept on a 12:12 light/dark cycle (lights on at 6:00 am), and received water and food *ad libitum.* Npas4 KO (*Npas4*$^{f/f}$) mice were previously described (Lin et al., 2008). All experimental procedures were performed on male mice. Pregnant rats purchased from Daehan Biolink were used *in vitro* for dissociated cultures of cortical or hippocampal neurons.

bioRxiv preprint doi: https://doi.org/10.1101/659805; this version posted June 4, 2019. The copyright holder for this preprint (which was not certified by peer review) is the author/funder. All rights reserved. No reuse allowed without permission.

METHOD DETAILS

Construction of Expression Vectors. *1*. IQSEC3. The shRNA lentiviral expression vector against mouse *Iqsec3* (Genbank accession number: NM_207617.1) was constructed by annealing, phosphorylating, and cloning oligonucleotides targeting mouse *Iqsec3* (5'-ACA TCA GAC CAT CGG CCA CGA CATT A-3') into the *Xho*I and *Xba*I sites of the L-315 vector [see (Ko et al., 2011) for a schematic diagram of the L-315 vector]. The shRNA AAV against mouse *Iqsec3* was constructed by cloning oligonucleotides identical to those used for subcloning into the pAAV-U6-GFP vector (Cell BioLabs, Inc.) using *BamH*I and *EcoR*I sites. AAVs encoding full-length rat *Iqsec3* WT and E749A point mutant were generated by amplification of the full-length region by PCR and subsequent subcloning into the pAAV-2A-tdTomato vector [a gift from Hailan Hu; (Li et al., 2013)] at *Xba*I and *BamH*I sites. *2*. Others. The shRNA lentiviral expression vector against *Bdnf* was constructed by annealing, phosphorylating, and cloning oligonucleotides targeting rat *Bdnf* (Genbank accession number: AY559250; 5'-ACA TCA GAC CAT CGG CCA CGA CATT A-3') into the *Xho*I and *Xba*I sites of the L-315 vector. The shRNA lentiviral expression vector against *Npas4* was constructed by annealing, phosphorylating, and cloning oligonucleotides targeting rat Npas4 (5′-GGT TGA CCC TGA TAA TTT A-3′) into the *Xho*I and *Xba*I sites of the L-315 vector. AAV encoding mouse *Bdnf* (Genbank accession

bioRxiv preprint doi: https://doi.org/10.1101/659805; this version posted June 4, 2019. The copyright holder for this preprint (which was not certified by peer review) is the author/funder. All rights reserved. No reuse allowed without permission.

number: AY231132) was generated by amplification of the full-length region by PCR and subsequent subcloning into the pAAV-2A-tdTomato vector at *Xba*I and *BamH*I sites. *3*. Previously published reagents. The following constructs were as previously described: myc-Npas4 [a gift from Yingxi Lin; (Lin et al., 2008)]; L-315 rat sh-IQSEC3, pcDNA3.1-Myc-IQSEC3 (shRNA-resistant) WT and E749A (Um et al., 2016); pAAV2/9-Cre-IRES-EGFP and pAAV2/9-ΔCre-IRES-EGFP (Xu and Sudhof, 2013); and pAAV2/9-WGA-Cre-IRES-tdTomato and pAAV2/9-WGA-ΔCre-IRES-tdTomato (Martinelli et al., 2016).

Antibodies. The following commercially available antibodies were used: goat polyclonal anti-EGFP (Rockland), goat polyclonal anti-Npas4 (Abcam), rabbit polyclonal anti-cholecystokinin-8 (Immunostar), mouse monoclonal anti-GAD67 (clone 1G10.2; Millipore), guinea pig polyclonal anti-VGLUT1 (Millipore), mouse monoclonal anti-gephyrin (clone 3B11; Synaptic Systems), rabbit polyclonal anti-$GABA_A$ receptor γ2 (Synaptic Systems), mouse monoclonal anti-PSD-95 (clone 7E3-1B8; Thermo Fischer Scientific), mouse monoclonal anti-β-actin (clone C4; Santa Cruz Biotechnology), mouse monoclonal anti-parvalbumin (clone PARV-19; Swant), and mouse monoclonal anti-somatostatin (clone YC7; Millipore). The following antibodies were previously described: rabbit polyclonal anti-IQSEC3 [JK079; (Um et al., 2016)]; guinea pig polyclonal anti-IQSEC3/SynArfGEF [a gift from Hiroyuki Sakagami; (Fukaya et al., 2011)];

bioRxiv preprint doi: https://doi.org/10.1101/659805; this version posted June 4, 2019. The copyright holder for this preprint (which was not certified by peer review) is the author/funder. All rights reserved. No reuse allowed without permission.

and rabbit polyclonal anti-Npas4 (Bloodgood et al., 2013).

***Iqsec3* Promoter-Luciferase Reporter Analysis.** A DNA fragment bracketing the proximal promoter and transcription start site of the *Iqsec3* gene (–280 to +36) was PCR-amplified from mouse genomic DNA and subcloned into the pGL3-Basic vector (Promega). Full-length mouse Npas4 cDNA was subcloned in pcDNA3 (Gibco-Invitrogen). For luciferase assays, 5×10^4 HEK293T cells in 24-well plates were transfected with an Npas4 expression vector and reporter plasmid using iN-fect (iNtRON Biotechnology). Cells were harvested after 48 hours and analyzed for luciferase activity as described by the manufacturer (Promega).

Electrophoretic Mobility Shift Assay. Full-length mouse Npas4 cDNA was subcloned into the pFASTBAC1 vector containing an N-terminal FLAG-tag, and baculovirus was generated according to the manufacturer's instructions (Thermo Fisher). After baculovirus infection into Sf9 insect cells, Npas4 protein was affinity purified on M2 agarose (Sigma) as described previously (Kim et al., 2009). An oligonucleotide containing the consensus sequence for Npas4 binding (5'-CGG GAA GCA GGG TTC CTC ACG AAG CCC AGA GGT GGG AGG TGG-3') and its point mutant (5'-CGG GAA GCA GGG TTC CTA AAA AAG CCC AGA GGT GGG AGG TGG-3'; mutated nucleotides are underlined) within the *Iqsec3* proximal promoter

bioRxiv preprint doi: https://doi.org/10.1101/659805; this version posted June 4, 2019. The copyright holder for this preprint (which was not certified by peer review) is the author/funder. All rights reserved. No reuse allowed without permission.

region were end-labeled using polynucleotide kinase and [γ-^{32}P]ATP and then annealed to complementary oligonucleotides. Reactions containing purified Npas4 protein in 19 µl of reaction buffer (10 mM Tris-Cl pH 7.5, 5 mM $MgCl_2$, 1 mM EDTA, 50 mM K-glutamate, 1 mM DTT and 5% glycerol) supplemented with 25 ng/µl poly (dI-dC) were pre-incubated on ice for 15 minutes. After addition of 1 µl of ^{32}P-labeled probe containing approximately 3 ng of oligonucleotide duplex, reactions were incubated on ice for 30 minutes. Protein in samples were resolved by electrophoresis at 4°C on 6% polyacrylamide gels in 0.25x TBE buffer and subjected to autoradiography.

Chromatin Immunoprecipitation Assays. Cultured cortical neurons at DIV14 were treated with 55 mM KCl for 6 hours, after which chromatin immunoprecipitation assays were performed according the manufacturer's instructions (Millipore). Detailed information about primers used for quantitative PCR is provided in **Table S1**.

Chemicals. Amino-5-phosphonopentanoic acid (D-APV; Cat. No. 0106), 2,3-dihydroxy-6-nitro-7-sulfamoyl-benzo[f] quinoxaline-2,3-dione (NBQX; Cat. No. 0373), 6,7-dinitroquinoxaline-2,3(1H,4H)-dione (DNQX; Cat. No. 0189), tetrodoxin (TTX; Cat. No. 1078), bicuculline (Cat. No. 0130), SecinH3 (Cat. No. 2849), QS11 (Cat. No. 3324), and QX-314 (Cat. No. 1014) were

bioRxiv preprint doi: https://doi.org/10.1101/659805; this version posted June 4, 2019. The copyright holder for this preprint (which was not certified by peer review) is the author/funder. All rights reserved. No reuse allowed without permission.

purchased from Tocris Bioscience. 6-Cyano-7-nitroquinoxaline-2,3-dione (CNQX; Cat. No. C239), picrotoxin (Cat. No. P1675), pilocarpine (Cat. No. P6503), methyl-scopolamine nitrate (Cat. No. S2250), 2,2,2-tribomoethyl alcohol (Cat. No. T4840-2), and Tert-amylalcohol (Cat. No. 24048-6), pentylenetetrazol (Cat. No. P6500), and kainic acid (Cat. No. K0250) were purchased from Sigma. Diazepam (Cat. No. 117) was purchased from Daewon Pharm.

Neuron Culture, Transfections, Imaging, and Quantitation. Cultured hippocampal neurons were prepared from E18 rat brains, as previously described (Ko et al., 2003b; Ko et al., 2006), cultured on coverslips coated with poly-D-lysine (Sigma), and grown in Neurobasal medium supplemented with B-27 (Thermo Fisher), 0.5% FBS (WELGENE), 0.5 mM Glutamax (Thermo Fisher), and sodium pyruvate (Thermo Fisher). For overexpression of IQSEC3 in cultured neurons, hippocampal neurons were transfected with pCAGGS-FLAG-IQSEC3 or its various derivatives, as indicated in the individual figures, or with EGFP (Control) using a CalPhos Transfection Kit (Takara) at DIV10 and immunostained at DIV14. For KD of IQSEC3 in cultured neurons, hippocampal neurons were transfected with L-315 alone (Control), L-315 rat sh-IQSEC3 (IQSEC3 KD), or cotransfected with IQSEC3 KD and shRNA-resistant myc-IQSEC3 using a CalPhos Transfection Kit (Takara) at DIV8 and immunostained at DIV14. The following drugs were used at the indicated concentrations in cultured neuron experiments: D-

bioRxiv preprint doi: https://doi.org/10.1101/659805; this version posted June 4, 2019. The copyright holder for this preprint (which was not certified by peer review) is the author/funder. All rights reserved. No reuse allowed without permission.

APV (100 μM), NBQX (20 μM), picrotoxin (50 μM), and KCl (55 mM). For immunocytochemistry, cultured neurons were fixed with 4% paraformaldehyde/4% sucrose, permeabilized with 0.2% Triton X-100 in phosphate buffered saline (PBS), immunostained with the indicated primary antibodies, and detected with the indicated Cy3- and fluorescein isothiocyanate (FITC)-conjugated secondary antibodies (Jackson ImmunoResearch). Images were acquired using a confocal microscope (LSM780, Carl Zeiss) with a 63 x objective lens; all image setting were kept constant. Z-stack images were converted to maximal intensity projection and analyzed to obtain the size, intensity, and density of puncta immunoreactivities derived from marker proteins. Quantification was performed in a blinded manner using MetaMorph software (Molecular Devices).

AAV Production, Stereotactic Surgery and Virus Injection. Recombinant AAVs were packaged with pHelper and AAV1.0 (serotype 2/9) capsids for high efficiency. HEK293T cells were cotransfected with pHelper and pAAV1.0, together with pAAV-U6-EGFP alone (Control), pAAV-U6-shNpas4 (Npas4 KD), pAAV-U6-sh-IQSEC3 (IQSEC3 KD), pAAV-IQSEC3 WT (+IQSEC3 WT), or pAAV-IQSEC3 E749A (+IQSEC3 DN). Cells were harvested 72–108 hours post transfection; after adding 0.5 M EDTA to the media, cells were washed three times with PBS, and collected by centrifugation. Cells were then resuspended in PBS and lysed by

bioRxiv preprint doi: https://doi.org/10.1101/659805; this version posted June 4, 2019. The copyright holder for this preprint (which was not certified by peer review) is the author/funder. All rights reserved. No reuse allowed without permission.

subjecting them to four freeze-thaw cycles in an ethanol/dry ice bath (7 minutes each) and 37°C water bath (5 minutes). Lysates were centrifuged and supernatants were collected and incubated with a solution containing 40% poly(ethylene glycol) (Sigma) and 2.5 M NaCl on ice for 1 hour and centrifuged at 2000 rcf for 30 minutes. The pellets were resuspended in HEPES buffer (20 mM HEPES pH 8.0, 115 mM NaCl, 1.2 mM $CaCl_2$, 1.2 mM $MgCl_2$, 2.4 mM KH_2PO_4), mixed with chloroform, and centrifuged at 400 rcf for 10 minutes. The supernatant was collected and concentrated using Amicon Ultra Centrifugal Filters (0.5 ml, 3K MWCO; Millipore). Viruses were assessed for infectious titer by RT-PCR, and used for infections at 1×10^{10}–10^{11} infectious units/μl. For stereotactic delivery of recombinant AAVs, 6–8-week-old C57BL/6N mice were anesthetized by inhalation of isoflurane (3–4%) or intraperitoneal injection of 2% Avertin solution (2,2,2-tribromoethyl alcohol dissolved in Tert-amylalcohol (Sigma)) dissolved in saline, and secured in the stereotactic apparatus. Viral solutions were injected with a Hamilton syringe using a Nanoliter 2010 Injector (World Precision Instruments) at a flow rate of 100 nl/min (injected volume, 0.6 μl). The coordinates used for stereotactic injections into mice are as follows: hippocampal DG injections (anterior-posterior [AP] -2.2 mm, medial-lateral [ML] ± 1.3 mm, and dorso-ventral [DV] 2.35 mm) and hippocampal CA1 injections (AP -2.2 mm, ML ± 1.3 mm, and DV 1.9 mm). Each injected mouse was returned to its home cage and used for scoring seizure-like behaviors, immunohistochemical analyses, electrophysiological recordings

bioRxiv preprint doi: https://doi.org/10.1101/659805; this version posted June 4, 2019. The copyright holder for this preprint (which was not certified by peer review) is the author/funder. All rights reserved. No reuse allowed without permission.

or behavioral analyses after 2–4 weeks.

***In Utero* Electroporation**. After anesthetizing pregnant ICR mice at 15 *days post coitum* (d.p.c) with an intraperitoneal injection of pentobarbital sodium (64.8 mg/kg), uterine horns were exposed through a longitudinal incision (~2 cm) in the abdomen. Approximately 1 μl of DNA solution containing 1 mg/ml pCAGGS-EGFP, 1.5 mg/ml L-315-IQSEC3 shRNA and 0.01% Fast Green in PBS, or 1 mg/ml pCAGGS-EGFP, 1.5 mg/ml L-315 control shRNA and 0.01% Fast Green in PBS was injected into the lateral ventricle of each embryo through a glass capillary electrode. The head of each embryo was placed between tweezer-type electrodes (CUY650P5; NEPA Gene). An anode of the electrode was placed on the injection side for the transfection of hippocampal CA1 pyramidal neurons. Square electric pulses (35 V, 50 ms) were administered four times at 1 Hz using an electroporator (CUY21; NEPA Gene). The uteri were returned to the peritoneal cavity, and the incisions were sutured. The operated mice were returned to their home cages and subsequently allowed to deliver naturally. The transfected pups were identified at P0 by visualizing the EGFP signals through the scalp using an LED penlight (Handy Blue; Reryon).

qRT-PCR. Cultured rat cortical neurons were infected with recombinant lentiviruses at DIV3

bioRxiv preprint doi: https://doi.org/10.1101/659805; this version posted June 4, 2019. The copyright holder for this preprint (which was not certified by peer review) is the author/funder. All rights reserved. No reuse allowed without permission.

and harvested at DIV10 for qRT-PCR using SYBR green qPCR master mix (Takara). Total RNA was extracted from rat cortical neurons using the TRIzol reagent (Invitrogen) according to the manufacturer's protocol. Briefly, one well of a 12-well plate of cultured neurons was harvested and incubated with 500 μl of TRIzol reagent at room temperature for 5 minutes. After phenol-chloroform extraction, RNA in the upper aqueous phase was precipitated. cDNA was synthesized from 500 ng of RNA by reverse transcription using a ReverTra Ace-α kit (Toyobo). Quantitative PCR was performed on a CFX96 Touch Real-Time PCR system (BioRad) using 1 μl of cDNA. The ubiquitously expressed β-actin was used as an endogenous control. The sequences of the primer pairs used are as follows: rat Iqsec3, 5'-GGA GCA GAT TCG GAT AGA ATG G-3' (forward) and 5'–GGG TGA TCC TTG CTT TGA CT-3' (reverse); rat Npas4, 5'-GAG GCT GGA CAT GGA TTT ACT–3' (forward) and 5'-GGG TGA TCC TTG CTT TGA CT-3' (reverse); rat Npas4, 5'-GAG GCT GGA CAT GGA TTT ACT-3' (forward) and 5'-CCT GGG TGT CTT CAG AGT TTA G-3' (reverse); rat Bdnf, 5'-CTG AGC GTG TGT GAC AGT ATT A-3' (forward) and 5'-CTT TGG ATA CCG GGA CTT TCT C-3'; rat Laf4, 5'-AAG CAA GGC GAG GAG AAT AG-3' (forward) and 5'-GCT TGA ATG GCG GAA AGT G-3'; mouse Npas4, 5'-CCT CCA AAG AGC TGG ACT TC-3' (forward) and 5'-ATC CTT GCT CAG GTC TGC TT-3' (reverse); mouse Iqsec3, 5'-ATC ACC ACC AAC ATC ACC AC–3' (forward) and 5'-CTT GAC AAT CTG CTG GCA CT-3' (reverse); and mouse gephyrin, 5'-CGG TGT ATA

bioRxiv preprint doi: https://doi.org/10.1101/659805; this version posted June 4, 2019. The copyright holder for this preprint (which was not certified by peer review) is the author/funder. All rights reserved. No reuse allowed without permission.

CTG ACT TGG CAT C-3' (forward) and 5'-CTC TGT CTT TGG AGG TAG CAT C-3' (reverse).

Animals. Animals were handled according to protocols approved by the DGIST Institutional Animal Care and Use Committee. Npas4 KO (*Npas4*$^{f/f}$) mice were previously described (Lin et al., 2008). Mice were provided *ad libitum* access to standard rodent chow and tap water, and were housed under a 12-hour light/dark cycle (lights off at 18:00).

Activity Alteration Protocols. *1. Electroconvulsive Seizure Stimulation.* ECS was administered to male C57BL/6N mice (n = mice/group) through ear clip electrodes (100 V, 0.5 s; Mecta VGO Basile ECT 7801). Control, sham-treated mice were treated the same as mice in the ECS group, except that electrical current was not administered. Mice were decapitated at predefined times (0, 3, and 6 hours) after treatment, and brains were frozen immediately. *2. Environmental Enrichment.* Male Npas4$^{f/f}$ mice (P28–P30) injected with AAV-ΔCre/EGFP (Control) or AAV-Cre/EGFP (Npas4 KO) into the CA1 region were kept for 4 weeks and then exposed to an enriched environment for 4–5 days before functional analyses. The enriched environment consisted of a large cage containing a running wheel, hut, tunnel and several other novel objects, as previously described (Sztainberg and Chen, 2010). *3. Dark Rearing Paradigm.* Male

bioRxiv preprint doi: https://doi.org/10.1101/659805; this version posted June 4, 2019. The copyright holder for this preprint (which was not certified by peer review) is the author/funder. All rights reserved. No reuse allowed without permission.

C57BL/6N mice were reared under a normal 12/12 hour light/dark cycle from birth until P26 (LR), or were transferred to a completely dark room at P21 (DR). The DR+2hL group was re-exposed to light for 2 hours before euthanization. Sections of the primary visual cortex or hippocampus were obtained and processed for qRT-PCR analyses. *4. Induced Seizure Protocols*. Seizures were induced by intraperitoneal administration of 11–12-week-old male mice with KA (15 mg/kg); saline injection was used as a control. Mice were decapitated at the indicated times (3 or 6 hours) after injection, and the injected mouse brains were prepared immediately for further analyses.

Immunohistochemistry. Three-month-old mice were anaesthetized and immediately perfused, first with PBS for 3 minutes, and then with 4% paraformaldehyde for 5 minutes. Brains were dissected out, fixed in 4% paraformaldehyde overnight, and then incubated with 30% sucrose (in PBS) overnight, and sliced into 30-μm-thick coronal sections using a vibratome (Model VT1200S; Leica Biosystems) or a cryotome (Model CM-3050-S; Leica Biosystems). Sections were permeabilized by incubating with 1% Triton X-100 in PBS containing 5% bovine serum albumen and 5% horse serum for 30 minutes. For immunostaining, sections were incubated for 8–12 hours at 4 °C with primary antibodies diluted in the same blocking solution. The following primary antibodies were used: anti-Npas4 (1:100), anti-IQSEC3 (JK079; 2 μg/ml), anti-GAD67

bioRxiv preprint doi: https://doi.org/10.1101/659805; this version posted June 4, 2019. The copyright holder for this preprint (which was not certified by peer review) is the author/funder. All rights reserved. No reuse allowed without permission.

(1:100), anti-PV (1:500), anti-CCK (1:100), and anti-SST (1:50). Sections were washed three times in PBS and incubated with appropriate Cy3- or FITC-conjugated secondary antibodies (Jackson ImmunoResearch) for 2 hours at room temperature. After three washes with PBS, sections were mounted onto glass slides (Superfrost Plus; Fisher Scientific) with Vectashield mounting medium (H-1200; Vector Laboratories).

***In vitro* and *Ex Vivo* Electrophysiology.** *1. In Vitro Electrophysiology*. Whole-cell patch-clamp recordings were obtained using DIV14–16 rat hippocampal cultured neurons transfected with the indicated plasmids using a calcium phosphate method. Recording patch pipettes (4–7 MΩ) were filled with an internal solution consisting of 90 mM Cs-gluconate, 10 mM CsCl, 10 mM HEPES, 10 mM EGTA, 5 mM NaCl, 4 mM Mg-ATP, and 0.3 mM Na-GTP (pH 7.2) for mEPSC recordings, and 100 mM CsCl, 10 mM HEPES, 10 mM EGTA, 5 mM NaCl, 4 mM Mg-ATP, and 0.3 mM Na-GTP (pH 7.2) for mIPSC recordings. Recordings were performed in HEPES-buffered saline solution (HBSS) with the following composition: 100 mM NaCl, 4 mM KCl, 1 mM NaH_2PO_4, 20 mM HEPES, 10 mM glucose, 2 mM $CaCl_2$, 1 mM $MgCl_2$, and 10 µM glycine. mEPSCs were recorded at a holding potential of -70 mV in the presence of 1 µM tetrodotoxin (TTX) to block action potentials, 100 µM picrotoxin to block $GABA_A$ receptors, and 50 µM APV to block NMDA receptors. mIPSCs were recorded at a holding potential

bioRxiv preprint doi: https://doi.org/10.1101/659805; this version posted June 4, 2019. The copyright holder for this preprint (which was not certified by peer review) is the author/funder. All rights reserved. No reuse allowed without permission.

of -70 mV in the presence of 1 µM TTX to block action potentials, 20 µM DNQX to block AMPA receptors, and 50 µM APV to block NMDA receptors. In each experiment, membrane statistics were monitored by collecting three 1-minute traces with a -2 mV voltage step between each trace. For all whole-cell recordings, membrane statistics were monitored after each trace. One criterion for whole-cell recordings was Ra < MΩ; in addition, cells were rejected if Ra or Rm changed by 20% or more over the course of the experiment. All recordings were digitized at 10 kHz and filtered at 2 kHz. Recordings were monitored with EPC10 USB double (HEKA) and analyzed offline using Mini Analysis (Synaptosoft). The experimenter was blinded to the identity of constructs throughout all data collection and analysis procedures. *2. Ex Vivo Electrophysiology*. Whole-cell voltage-clamp recordings were obtained from acute brain slices. Brain slices were transferred to a recording chamber and perfused with a bath solution of aerated (O_2 95%/CO_2 5% mixed gas) artificial cerebrospinal fluid (aCSF) consisting of 124 mM NaCl, 3 mM KCl, 1.3 mM $MgSO_4$, 1.25 mM NaH_2PO_4, 26 mM $NaHCO_3$, 2.4 mM $CaCl_2$-$2H_2O$, and 10 mM glucose at 32°C. Patch pipettes (open pipette resistance, 2–5 MΩ) were filled with an internal solution consisting of 130 mM CsCl, 2 mM $NgCl_2$, 10 mM HEPES, 5 mM Mg-ATP, 0.5 mM Na-GTP and 0.1 mM EGTA. For experiments in which eIPSCs were recorded, currents were pharmacologically isolated by bath application of 50 µM D-APV (Tocris) and 50 µM CNQX (Sigma), and inclusion of 5 mM QX-314 (Sigma) in the internal solution.

bioRxiv preprint doi: https://doi.org/10.1101/659805; this version posted June 4, 2019. The copyright holder for this preprint (which was not certified by peer review) is the author/funder. All rights reserved. No reuse allowed without permission.

Responses in hippocampal CA1 pyramidal neurons in the pyramidal layer evoked by stimulation of neurons in the SR layer were measured from a holding potential of -70 mV. Extracellular stimulation within specific layers of the hippocampus was achieved by current injection through a stimulating electrode placed in the relevant layer within 100–200 μm laterally of the patched pair. The stimulus strength used was the minimum required to generate an eIPSC in both Npas4 WT and Npas4 KO neurons. Electrophysiological data were acquired using pCLAMP software and a MultiClamp 700B (Axon Instruments), and were digitized using an Axon DigiData 1550B data acquisition board (Axon Instruments). Data were sampled at 10 kHz and filtered at 4 kHz. Experiments were discarded if the holding current was greater than -500 pA, the mean series resistance of pairs was greater than 30 MΩ, or if the series resistance differed by more than 30% between the two recordings. In experiments in which direct comparisons were made between two neurons, all data were normalized to the peak amplitude of Npas4 WT neurons. The amplitude of eIPSCs was calculated by averaging the normalized peak amplitude. Paired-pulse ratios were calculated by recording the amplitudes of paired eIPSC at stimulation intervals of 25, 50, 100 and 200 ms.

Mouse Behavioral Tests. Male Npas4$^{f/f}$ mice (9–11 weeks old) injected with AAV-ΔCre/EGFP (Control) or AAV-Cre/EGFP (Npas4 KO) into the CA1 region were used for all behavioral tests.

bioRxiv preprint doi: https://doi.org/10.1101/659805; this version posted June 4, 2019. The copyright holder for this preprint (which was not certified by peer review) is the author/funder. All rights reserved. No reuse allowed without permission.

Tests were performed in the following order: Y-maze, open-field, novel object-recognition, elevated-plus maze, and forced swim test. Mice were excluded for quantitative analyses if one or both of the injections were off-target, as demonstrated by *post hoc* immunostaining after behavioral analyses.

Behavioral Analyses. *1. Y-maze test.* A Y-shaped white acrylic maze with three 40-cm–long arms at a 120° angle from each other was used. Mice were introduced into the center of the maze and allowed to explore freely for 8 minutes. An entry was counted when all four limbs of a mouse were within the arm. The movement of mice was recorded by a top-view infrared camera, and analyzed using EthoVision XT 10 software (Noldus). *2. Open-field test.* Mice were placed into a white acrylic open-field box (40 × 40 × 40 cm), and allowed to freely explore the environment for 60 minutes in the dark (0 lux). The traveled distance moved and time spent in the center zone of freely moving mice were recorded by a top-view infrared camera, and analyzed using EthoVision XT 10 software (Noldus). *3. Novel object-recognition test.* An open field chamber was used in this test. Mice were habituated to the chamber for 10 minutes. For training sessions, two identical objects were placed in the center of the chamber at regular intervals, and mice were allowed to explore the objects for 10 minutes. After the training session, mice were returned to their home cage for 6 hours. For novel object-recognition tests,

bioRxiv preprint doi: https://doi.org/10.1101/659805; this version posted June 4, 2019. The copyright holder for this preprint (which was not certified by peer review) is the author/funder. All rights reserved. No reuse allowed without permission.

one of the two objects was exchanged for a new object, placed in the same position of the chamber. Mice were returned to the chamber and allowed to explore freely for 10 minutes. The movement of mice was recorded by infrared camera, and the number and duration of contacts were analyzed using EthoVision XT 10 (Noldus). *4. Elevated plus-maze test.* The elevated plus-maze is a plus-shaped (+) white acrylic maze with two open arms (30 × 5 × 0.5 cm) and two closed arms (30 × 5 × 30 cm) positioned at a height of 75 cm from the floor. Light conditions around open and closed arms were ~300 and ~30 lux, respectively. For the test, mice were introduced into the center zone of the elevated plus-maze and allowed to move freely for 10 minutes. All behaviors were recorded by a top-view infrared camera, and the time spent in each arm and the number of arm entries were measured and analyzed using EthoVision XT 10 software (Noldus). *5. Forced swim test.* Mice were individually placed in a glass cylinder (15 × 30 cm) containing water (24°C ± 1°C; depth, 15 cm). All mice examined were forced to swim for 6 minutes, and the duration of immobility was recorded and measured during the final 4 minutes of the test. The latency to immobility from the start of the test (delay between the start of the test and appearance of the first bout of immobility, defined as a period of at least 1 second without any active escape behavior), and the duration of immobility (defined as the time not spent actively exploring the cylinder or trying to escape from it) were measured. Immobility time was defined as the time the mouse spent floating in the water without struggling, making

bioRxiv preprint doi: https://doi.org/10.1101/659805; this version posted June 4, 2019. The copyright holder for this preprint (which was not certified by peer review) is the author/funder. All rights reserved. No reuse allowed without permission.

only minor movements that were strictly necessary to maintain its head above water.

QUANTIFICATION AND STATISTICAL ANALYSES

Data Analysis and Statistics.

All data are expressed as means ± SEM. All experiments were repeated using at least three independent cultures, and data were statistically evaluated using a Mann-Whitney *U* test, analysis of variance (ANOVA) followed by Tukey's *post hoc* test, Kruskal-Wallis test (one-way ANOVA on ranks), paired two-tailed t-test (for electrophysiology experiments), or one-way ANOVA with Bonferroni's *post hoc* test (for behavior experiments), as appropriate. Prism7 (GraphPad Software) was used for analysis of data and preparation of bar graphs. P-values < 0.05 were considered statistically significant (individual p-values are presented in figure legends).

Figure 1

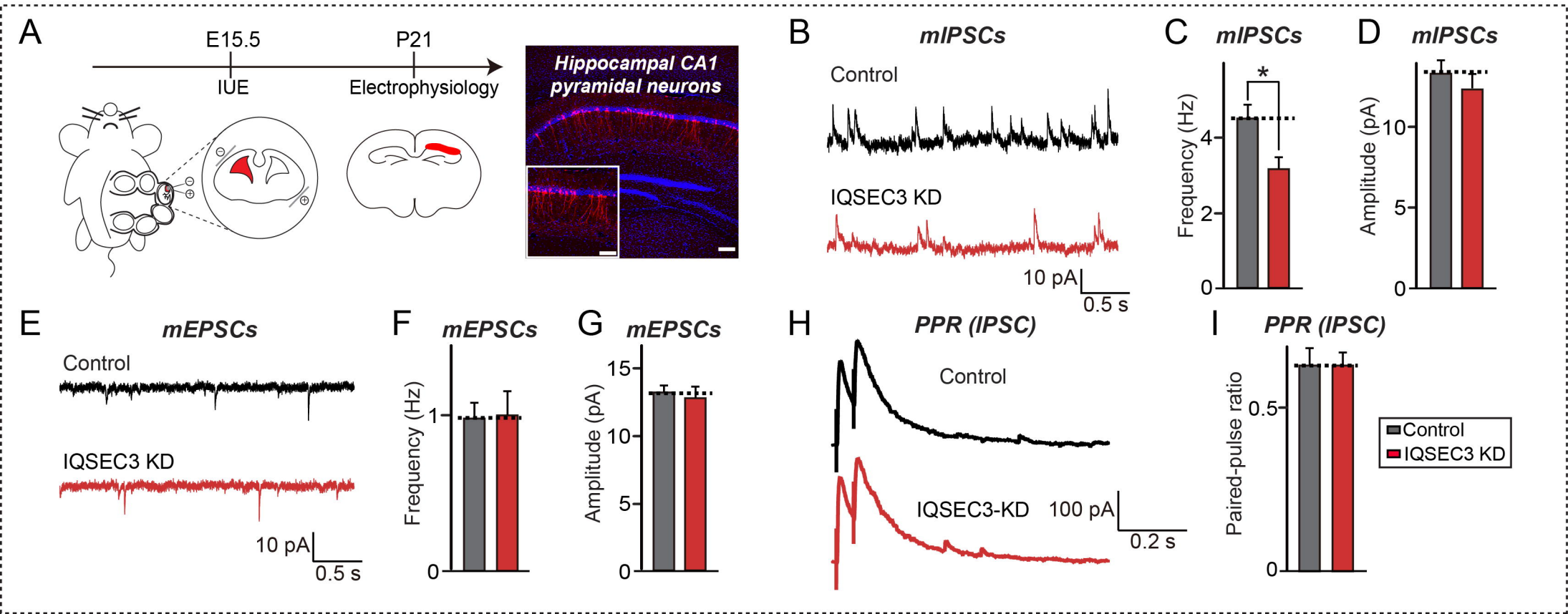
A
E15.5
IUE
P21
Electrophysiology
Hippocampal CA1 pyramidal neurons
B
mIPSCs
Control
IQSEC3 KD
10 pA
0.5 s
C
mIPSCs
Frequency (Hz)
*
D
mIPSCs
Amplitude (pA)
E
mEPSCs
Control
IQSEC3 KD
10 pA
0.5 s
F
mEPSCs
Frequency (Hz)
G
mEPSCs
Amplitude (pA)
H
PPR (IPSC)
Control
IQSEC3-KD
100 pA
0.2 s
I
PPR (IPSC)
Paired-pulse ratio
Control
IQSEC3 KD

Figure 2

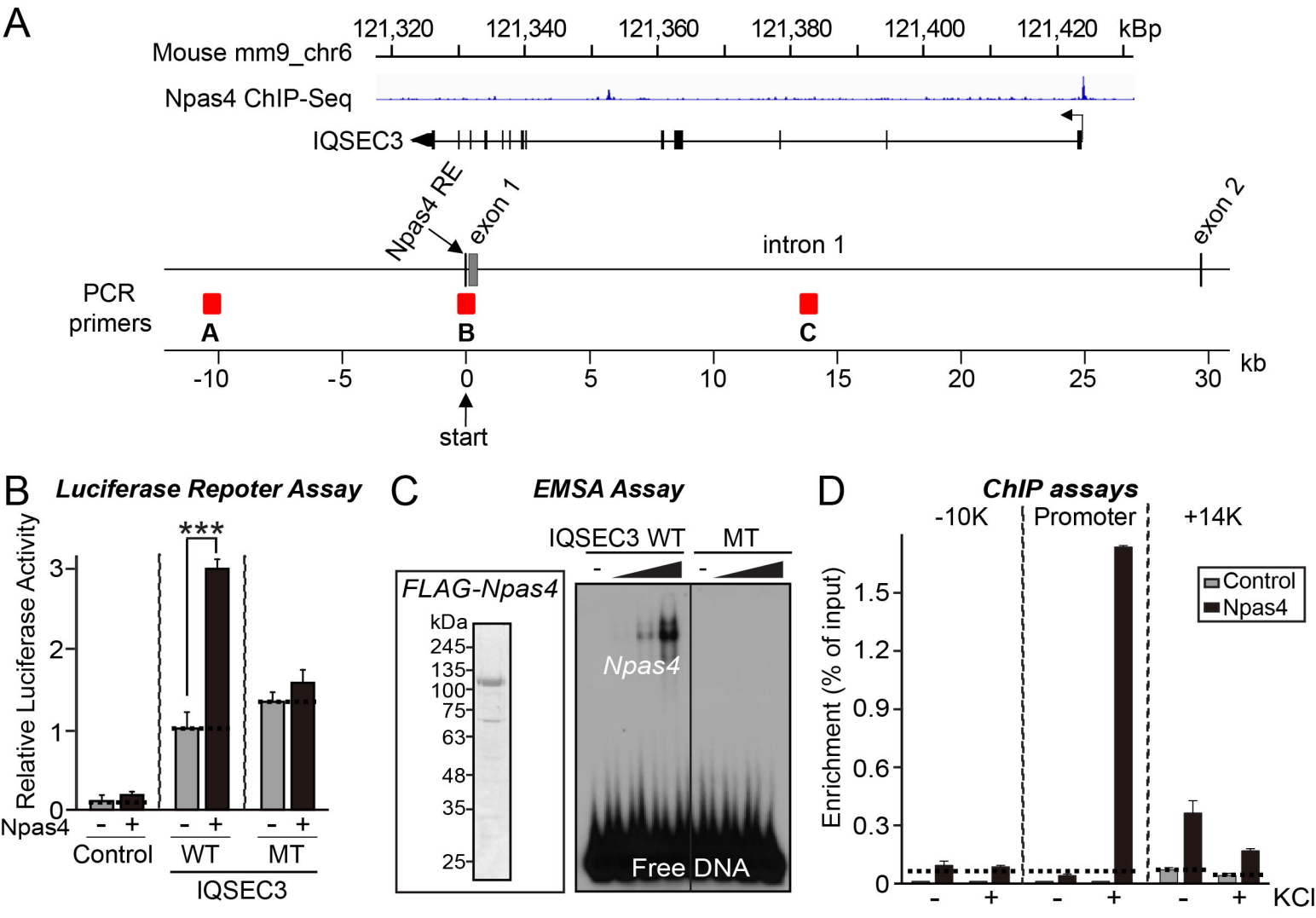
A
121,320
121,340
121,360
121,380
121,400
121,420
kBp
Mouse mm9_chr6
Npas4 ChIP-Seq
IQSEC3
Npas4 RE
exon 1
intron 1
exon 2
PCR primers
A
B
C
-10
-5
0
5
10
15
20
25
30
kb
start
B
Luciferase Repoter Assay
Relative Luciferase Activity
***
Npas4
Control
WT
MT
IQSEC3
C
EMSA Assay
IQSEC3 WT
MT
FLAG-Npas4
kDa
245
135
100
75
63
48
35
25
Npas4
Free DNA
D
ChIP assays
-10K
Promoter
+14K
Control
Npas4
Enrichment (% of input)
KCl

Figure 3

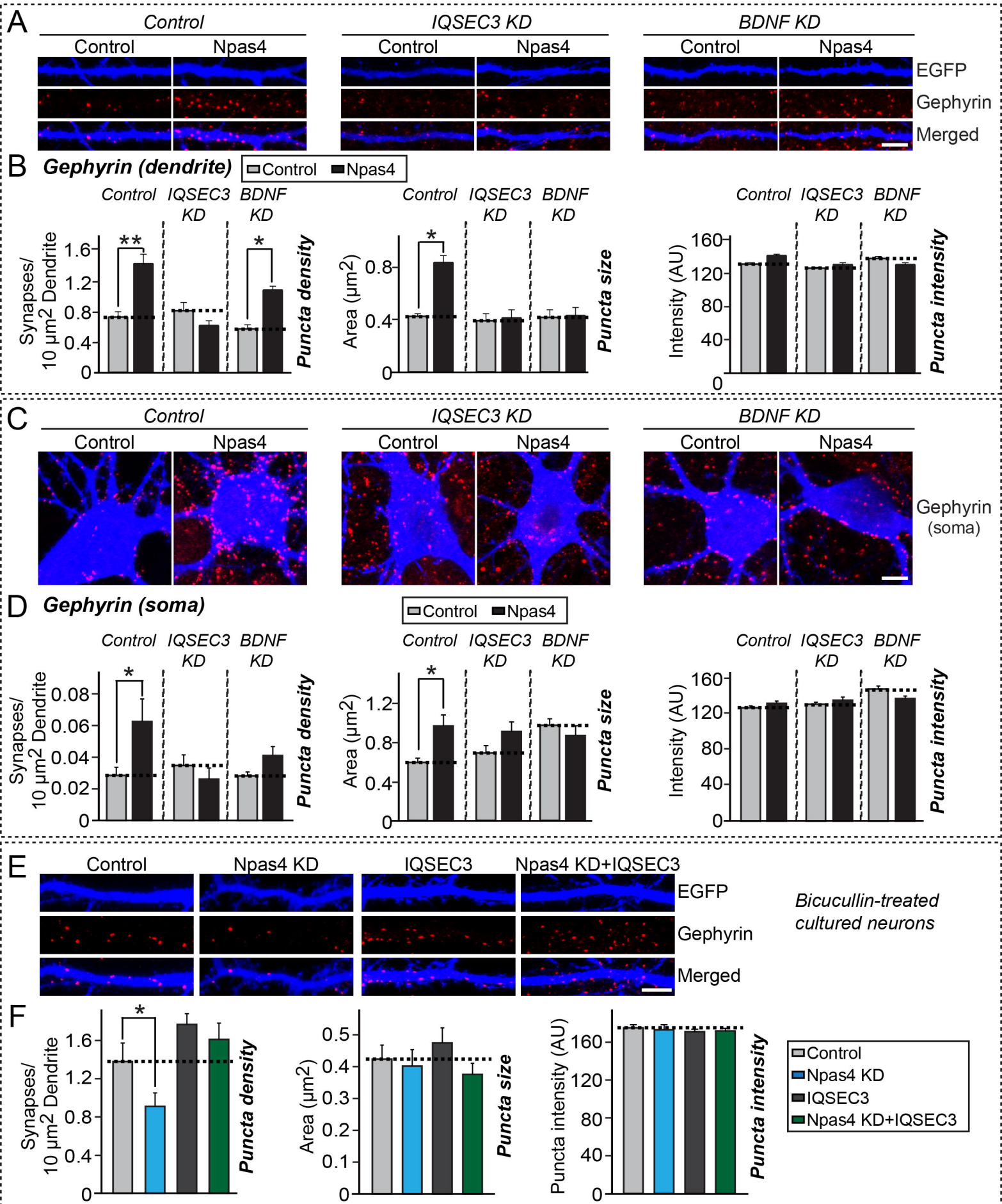
A
Control
IQSEC3 KD
BDNF KD
Control
Npas4
EGFP
Gephyrin
Merged
B
Gephyrin (dendrite)
Control
Npas4
Synapses/ 10 µm2 Dendrite
Puncta density
Area (µm2)
Puncta size
Intensity (AU)
Puncta intensity
C
Gephyrin (soma)
D
Gephyrin (soma)
E
Control
Npas4 KD
IQSEC3
Npas4 KD+IQSEC3
EGFP
Gephyrin
Merged
Bicucullin-treated cultured neurons
F
Puncta intensity (AU)
Npas4 KD
IQSEC3
Npas4 KD+IQSEC3

Figure 4

bioRxiv preprint doi: https://doi.org/10.1101/659805; this version posted June 4, 2019. The copyright holder for this preprint (which was not certified by peer review) is the author/funder. All rights reserved. No reuse allowed without permission.

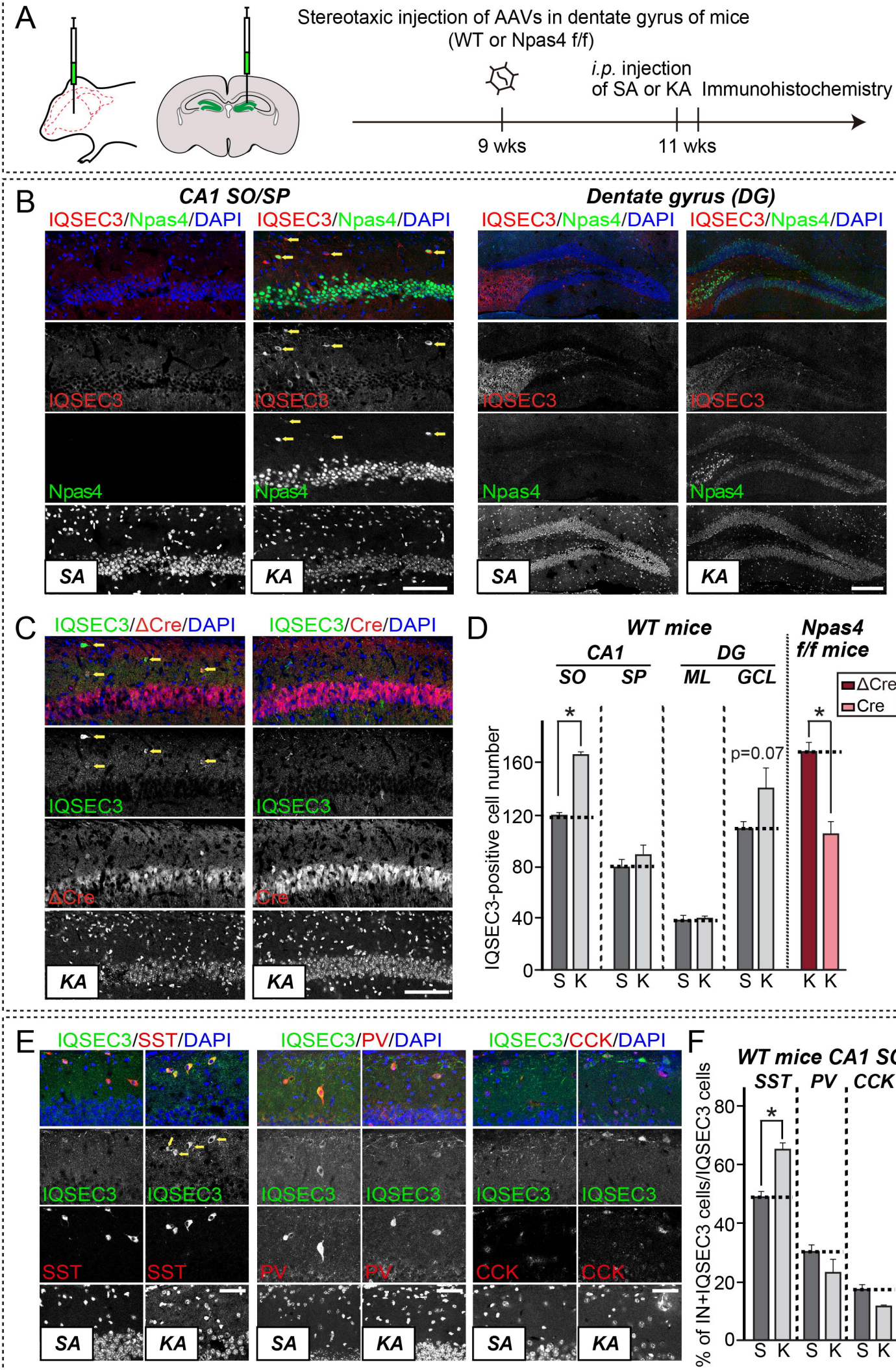

Figure 5

bioRxiv preprint doi: https://doi.org/10.1101/666065; this version posted June 4, 2019. The copyright holder for this preprint (which was not certified by peer review) is the author/funder. All rights reserved. No reuse allowed without permission.

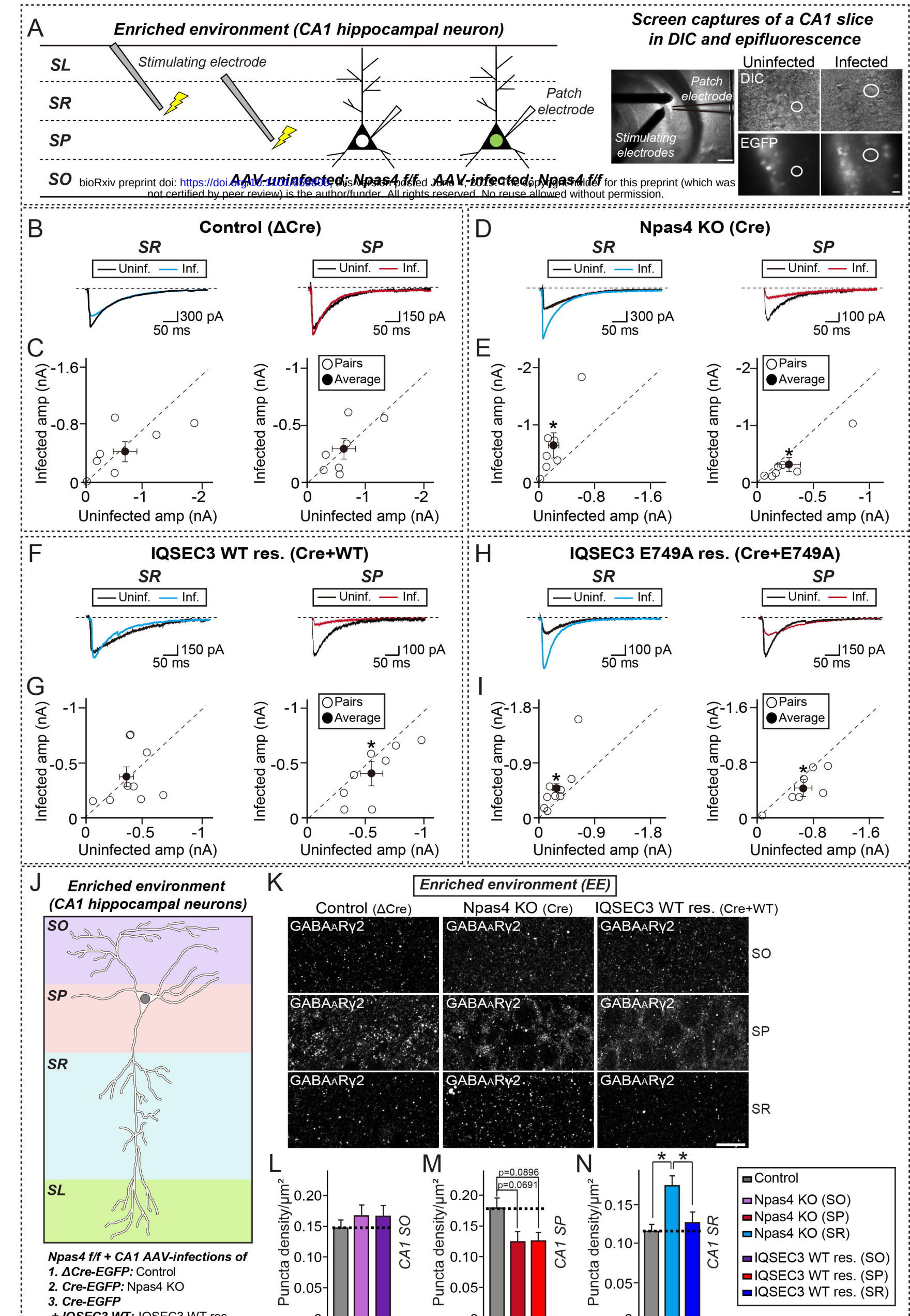

Figure 6

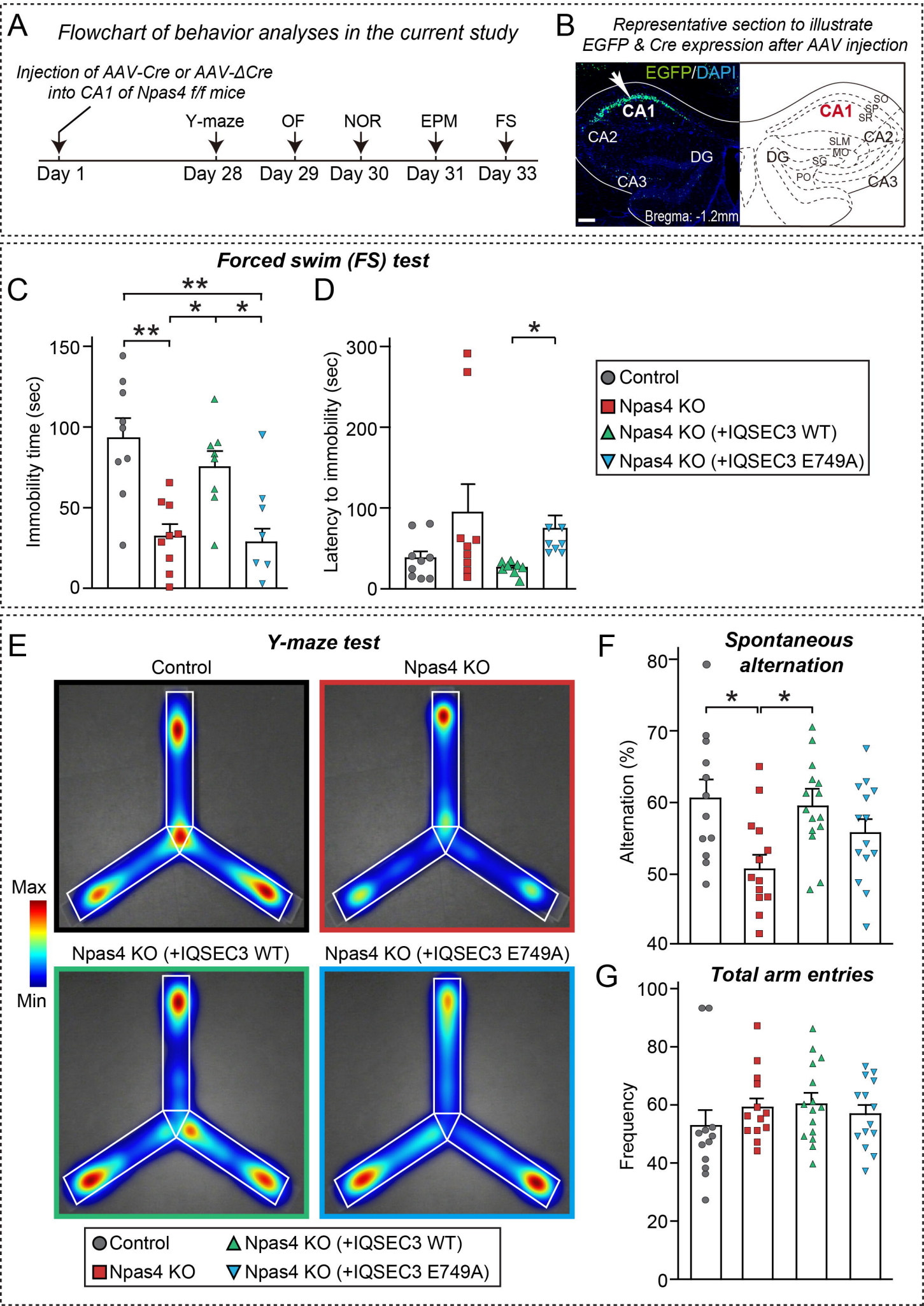
A
Flowchart of behavior analyses in the current study
Injection of AAV-Cre or AAV-ΔCre into CA1 of Npas4 f/f mice
Y-maze
OF
NOR
EPM
FS
Day 1
Day 28
Day 29
Day 30
Day 31
Day 33
B
Representative section to illustrate EGFP & Cre expression after AAV injection
EGFP/DAPI
CA1
CA2
DG
CA3
Bregma: -1.2mm
SO
SP
SR
SLM
MO
SG
PO
Forced swim (FS) test
C
Immobility time (sec)
D
Latency to immobility (sec)
Control
Npas4 KO
Npas4 KO (+IQSEC3 WT)
Npas4 KO (+IQSEC3 E749A)
E
Y-maze test
Max
Min
F
Spontaneous alternation
Alternation (%)
G
Total arm entries
Frequency

Figure 7

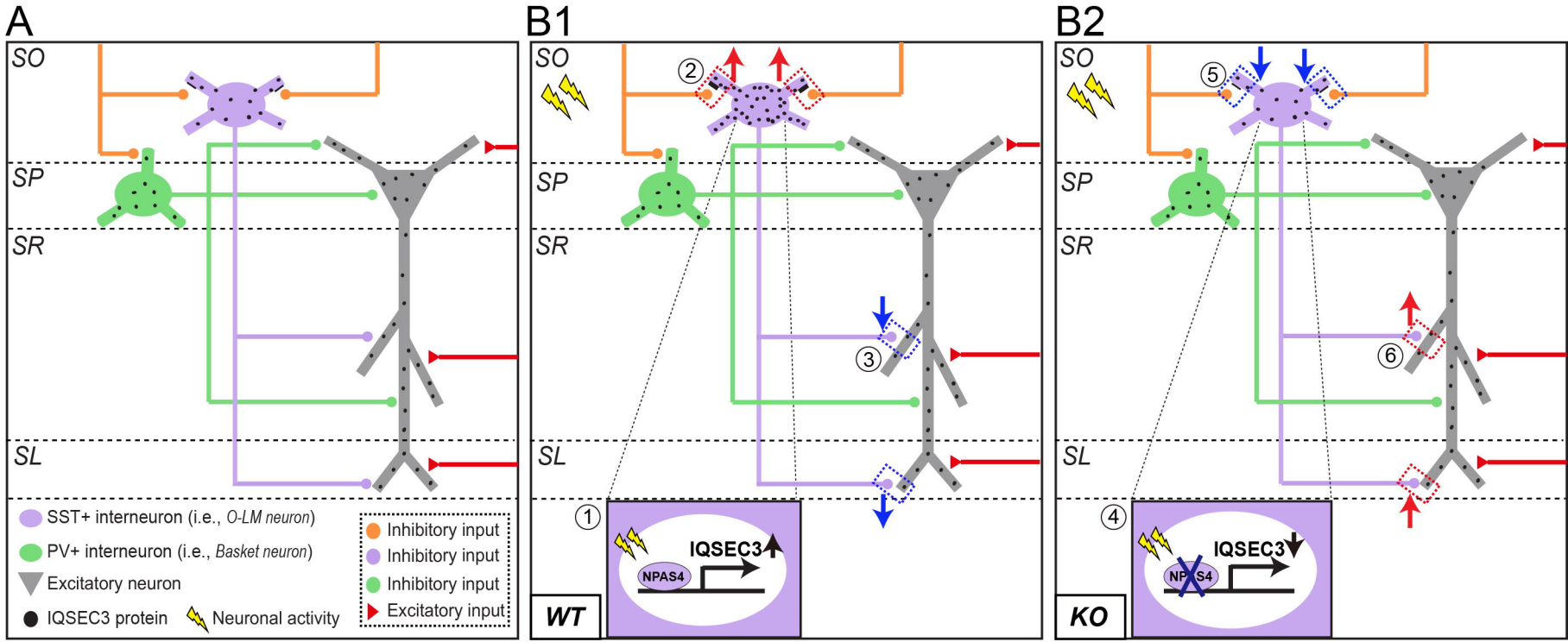
A
B1
B2
SO
SP
SR
SL
SST+ interneuron (i.e., O-LM neuron)
PV+ interneuron (i.e., Basket neuron)
Excitatory neuron
IQSEC3 protein
Neuronal activity
Inhibitory input
Inhibitory input
Inhibitory input
Excitatory input
①
②
③
④
⑤
⑥
IQSEC3
NPAS4
WT
KO
Npas4-independent IQSEC3 action
Npas4-dependent IQSEC3 action